Published in "The Journal of Comparative Neurology 511(4):
497 - 520, 2008" which should be cited to refer to this work.

Intrinsic Connections of the Macaque Monkey Hippocampal Formation: I. Dentate Gyrus

HIDEKI KONDO,[1] PIERRE LAVENEX,[1,2] AND DAVID G. AMARAL[1]*

[1]Department of Psychiatry and Behavioral Sciences, The M.I.N.D. Institute, The Center for Neuroscience and the California National Primate Research Center, University of California, Davis, Davis, California 95817

[2]Department of Medicine, Unit of Physiology, University of Fribourg, 1700 Fribourg, Switzerland

ABSTRACT

We have carried out a detailed analysis of the intrinsic connectivity of the *Macaca fascicularis* monkey hippocampal formation. Here we report findings on the topographical organization of the major connections of the dentate gyrus. Localized anterograde tracer injections were made at various rostrocaudal levels of the dentate gyrus, and we investigated the three-dimensional organization of the mossy fibers, the associational projection, and the local projections. The mossy fibers travel throughout the transverse extent of CA3 at the level of the cells of origin. Once the mossy fibers reach the distal portion of CA3, they change course and travel for 3–5 mm rostrally. The associational projection, originating from cells in the polymorphic layer, terminates in the inner one-third of the molecular layer. The associational projection, though modest at the level of origin, travels both rostrally and caudally from the injection site for as much as 80% of the rostrocaudal extent of the dentate gyrus. The caudally directed projection is typically more extensive and denser than the rostrally directed projection. Cells in the polymorphic layer originate local projections that terminate in the outer two-thirds of the molecular layer. These projections are densest at the level of the cells of origin but also extend several millimeters rostrocaudally. Overall, the topographic organization of the intrinsic connections of the monkey dentate gyrus is largely similar to that of the rat. Such extensive longitudinal connections have the potential for integrating information across much of the rostrocaudal extent of the dentate gyrus.

Indexing terms: hippocampus; mossy fibers; associational projection; CA3; granule cells; mossy cells

The hippocampal formation comprises a group of cortical regions, including the dentate gyrus, hippocampus, subiculum, presubiculum, parasubiculum, and entorhinal cortex (Amaral and Lavenex, 2007). Damage to these structures in adult humans and animals causes a profound loss of declarative memory function, without other sensory, motor, or cognitive impairments (Milner et al., 1998). Indeed, hippocampal damage causes episodic memory deficit in adult humans (Squire and Zola, 1996) and prevents the elaboration of spatial relational memory, a fundamental component of episodic memory, in adult nonhuman primates (Banta-Lavenex et al., 2006).

The hippocampal formation comprises a unique set of unidirectional excitatory pathways (Amaral and Lavenex, 2007). The entorhinal cortex provides the major input to the dentate gyrus, which does not return a projection to the entorhinal cortex. The dentate gyrus, in turn, projects to the CA3 field of the hippocampus. Moreover, the unique intrinsic neuroanatomy of the dentate gyrus elucidated in rats predicts that it carries out a specific information-

Grant sponsor: National Institutes of Health; Grant number: R01-NS16980 (to D.G.A.); Grant sponsor: Swiss National Science Foundation; Grant number: PP00A-106701 (to P.L.).

*Correspondence to: David G. Amaral, PhD, The M.I.N.D. Institute, University of California, Davis, 2825 50th Street, Sacramento, CA 95817. E-mail: dgamaral@ucdavis.edu

processing task with the information that it receives from the entorhinal cortex and ultimately conveys to CA3. However, the neuroanatomical organization of the major connections of the primate dentate gyrus, namely, the mossy fibers, the associational projection, and the local projections, has undergone relatively meager investigation (Rosene and Van Hoesen, 1977). Without such information, it is impossible to evaluate whether the fundamental principles of neuroanatomical organization are conserved between species or whether functional information derived from rodent studies can be applied or even extrapolated to monkeys or humans.

Previous studies have provided a thorough description of the neuroanatomical organization of the mossy fibers, associational projections, and local projection of the dentate gyrus in the rat (Blackstad et al., 1970; Zimmer, 1971; Fricke and Cowan, 1978; Gaarskjaer, 1978, 1981; Swanson et al., 1978; Laurberg and Sorensen, 1981; Bakst et al., 1986; Claiborne et al., 1986; Amaral and Witter, 1989; Buckmaster and Schwartzkroin, 1995; Buckmaster et al., 1996). The granule cells of the dentate gyrus give rise to mossy fibers that terminate on a number of neuronal types both within the polymorphic layer of the dentate gyrus and within the CA3 field of the hippocampus. Mossy fibers terminate with specialized large presynaptic terminals on the proximal dendrites of mossy cells in the polymorphic layer and on the proximal dendrites of the pyramidal cells of the CA3 region of the hippocampus (Blackstad et al., 1970; Amaral, 1978, 1979; Gaarskjaer, 1978, 1981; Amaral and Dent, 1981; Ribak et al., 1985; Claiborne et al., 1986; Frotscher et al., 1991; Acsady et al., 1998). Mossy fibers also have thinner collaterals that give rise to typically sized presynaptic boutons, and these terminate preferentially on γ-aminobutyric acid (GABA)-ergic neurons in the polymorphic layer and CA3 region (Amaral, 1978; Frotscher, 1989; Acsady et al., 1998; Seress et al., 2001). The mossy fibers innervate substantially greater numbers of inhibitory than excitatory cells in both the polymorphic layer and CA3 (Acsady et al., 1998; Seress et al., 2001). The mossy fibers are thought to use glutamate as a primary transmitter (Storm-Mathisen and Fonnum, 1972), although they colocalize GABA (Sandler and Smith, 1991) and a number of peptides, including dynorphin (Gall, 1984; van Daal et al., 1989).

In the rat, mossy fibers run transversely at approximately the same septotemporal level as the cells of origin and forms the stratum lucidum located superficially to the pyramidal cell layer (Gaarskjaer, 1978; Swanson et al., 1978; Claiborne et al., 1986). In the proximal portion of CA3, additional fibers run both below (infrapyramidal bundle) and within (intrapyramidal bundle) the pyramidal cell layer. At the distal part of CA3, the mossy fibers make an abrupt turn temporally and travel parallel to the long axis of the hippocampus (Gaarskjaer, 1978, 1981; Swanson et al., 1978; Amaral and Witter, 1989; Buckmaster et al., 2002). Swanson et al. (1978) reported that the mossy fibers arising from granule cells located at septal levels travel for approximately 2 mm in the temporal direction (approximately 20% of the full septotemporal length of the rat hippocampus), whereas they found a shorter longitudinal component from granule cells located at more temporal levels of the dentate gyrus. In contrast, Gaarskjaer (1978) observed the same amount of temporally directed mossy fiber projection regardless of the septotemporal level of the injection site.

The associational projection, which originates mainly from the mossy cells in the polymorphic layer of the dentate gyrus, terminates in the inner one-third of the molecular layer of the dentate gyrus (Zimmer, 1971; Amaral, 1978; Fricke and Cowan, 1978; Swanson et al., 1978; Laurberg, 1979; Laurberg and Sorensen, 1981; Amaral and Witter, 1989; Buckmaster et al., 1992, 1996; Blasco-Ibanez and Freund, 1997; Buckmaster and Amaral, 2001; Seress et al., 2008). The mossy cells receive asymmetric synaptic contacts from the mossy fibers of the granule cells (Amaral, 1978; Ribak et al., 1985; Frotscher et al., 1991; Blasco-Ibanez and Freund, 1997). Thus, the associational projection constitutes an excitatory feedback circuit with the granule cells. Several studies have demonstrated that the associational projection is distributed widely, both temporally and septally, from the cells of origin (Fricke and Cowan, 1978; Swanson et al., 1978; Amaral and Witter, 1989; Buckmaster et al., 1996). In rats, the associational projection is part of a collateral system of fibers that also contributes a contralaterally directed commissural projection that terminates in the same portion of the molecular layer (Blackstad, 1956; Hjorth-Simonsen and Laurberg, 1977; Laurberg, 1979; Laurberg and Sorensen, 1981; Swanson et al., 1981).

Amaral and Witter (1989) found that the associational projection from midseptotemporal levels travels for approximately 7 mm septotemporally (that is, for about 70% of the length of the rat hippocampus). They also reported that the associational projection is either not present or very weak at the level of the injection site. The projection begins to innervate the molecular layer at a distance of approximately 1 mm away from the injection site, and the heaviest terminal labeling occurs as much as 2–3 mm from the first indication of the projection. Injections into the septal one-third of the rat dentate gyrus reveal extensive projections throughout the septal half of the dentate gyrus. Injections into midseptotemporal levels result in labeling throughout the septal two-thirds of the dentate gyrus (Fricke and Cowan, 1978; Swanson et al., 1978). The associational projection arising from temporal portions of the dentate gyrus, however, is confined to the temporal one-third (Zimmer, 1971; Fricke and Cowan, 1978; Swanson et al., 1978).

Beyond the mossy fiber and associational connections, a population of polymorphic layer cells, some of which colocalize GABA and somatostatin, give rise to projections to the outer molecular layer (Bakst et al., 1986; Amaral and Witter, 1989; Leranth et al., 1990; Buckmaster and Schwartzkroin, 1995; Katona et al., 1999; Buckmaster et al., 2002). These projections are heaviest at the level of the cells of origin (Amaral and Witter, 1989; Buckmaster and Schwartzkroin, 1995). The term *local connection* for these projections is somewhat of a misnomer, insofar as it has been demonstrated in rodents that some of the interneurons that give rise to the local projection in the outer molecular layer have axons that extend for up to half of the total septotemporal length of the dentate gyrus (Buckmaster and Schwartzkroin, 1995; Buckmaster et al., 2002). The somatostatin/GABA cells receive excitatory inputs from the granule cells and send inhibitory projections back to the dendrites of the granule cells (Leranth et al., 1990; Katona et al., 1999). Thus, in rats, the local projections constitute mainly an inhibitory feedback circuit with the granule cells.

There are only a few published studies of these connections in the monkey dentate gyrus (Rosene and Van Hoesen, 1977, 1987; Buckmaster and Amaral, 2001). Rosene and Van Hoesen used ^{3}H-amino acid autoradiography to demonstrate that the dentate gyrus gives rise to projections to the CA3 region of the hippocampus (Rosene and Van Hoesen, 1977, 1987) and to its own inner molecular layer (Rosene and Van Hoesen, 1987). Buckmaster and Amaral (2001), using an intracellular labeling method, demonstrated that mossy cells in the monkey dentate gyrus send axonal projections to the inner molecular layer and that interneurons located in the polymorphic layer project to the outer molecular layer. However, the question remains whether the major principles of the topographical organization observed for the connections of the rat dentate gyrus can be applied to the primate brain (Amaral et al., 2007). We analyzed the intrinsic connectivity of the macaque monkey hippocampal formation using the discrete anterograde tracers *Phaseolus vulgaris*-leucoagglutinin (PHA-L) and biotinylated dextran amine (BDA) as well as the retrograde tracer cholera toxin B subunit (CTB). In this first report, we describe the topographical organization of the major connections of the macaque monkey dentate gyrus, namely, the mossy fibers, the associational projection, and the local projections.

MATERIALS AND METHODS

Surgery

All surgical and experimental procedures were approved by the UC Davis Animal Care and Use Committee and conform to NIH guidelines. Nineteen *Macaca fascicularis* monkeys of either sex, between 4 and 18 years of age and weighing 3–8 kg at the time of surgery, were used in these studies.

For all monkeys that underwent surgery between 2001 and 2003, magnetic resonance imaging (MRI) scans were performed prior to surgery to define the surgical coordinates for tracer injections. Monkeys were anesthetized with ketamine hydrochloride (15 mg/kg i.m.) and medetomidine (30 μg/kg) and placed in an MRI-compatible stereotaxic apparatus (Crist Instruments Co., Damascus, MD). Brain images were acquired on a General Electric 1.5-T Gyroscan magnet; 1.00-mm-thick sections were taken using a T1-weighted inversion recovery pulse sequence (TR = 21, TE = 7.9, NEX 4, FOV = 16 cm, matrix 256 × 256). The MRI images were analyzed, and a stereotaxic atlas was prepared to determine the coordinates for injection of the neuroanatomical tracers. For all monkeys that underwent surgery in 1992–1993, the standard atlas of Szabo and Cowan (1984) was used to determine the coordinates for injection of the neuroanatomical tracers.

For surgery, animals were preanesthetized with ketamine hydrochloride (8 mg/kg i.m.), intubated with a tracheal cannula, and mounted in a stereotaxic apparatus. The animals were then placed on a mechanical ventilator with which a surgical level of anesthesia was maintained with a combination of isoflurane (1%) and intravenous infusion of fentanyl (7–10 μg/kg/hour), or isoflurane alone (1–3% as needed) for cases in 2001–2003 and with isoflurane (1%) alone for cases in 1992–1993. With sterile procedures, the skull was exposed, and a small hole was made at a site appropriate for the injection. Electrophysiological recordings were performed to confirm the appropriate dorsoventral coordinate for placement of the injection. Neuroanatomical tracers were iontophoretically injected (see below). After the last injection, the wound was sutured in three layers, and the animal recovered from anesthesia. Analgesics (0.15 mg/kg oxymorphone given three times daily or 0.02 mg/kg buprenorphine twice daily) were administered immediately postsurgically. A prophylactic regime of antibiotics (20 mg/kg Cefazolin three times daily) was also administered during the first 5 days of the survival period.

Neuroanatomical tracer injections

Each monkey received up to two different, discrete, anterograde tracer injections of PHA-L (Vector Laboratories, Burlingame, CA; 2.5% solution in 0.1 M PO_4 buffer, pH 7.4; N = 7) or BDA (Molecular Probes, Eugene, OR; 10% solution in 0.1 M PO_4 buffer, pH 7.4; N = 7) into various rostrocaudal and transverse portions of the dentate gyrus (one on each side of the brain), and some monkeys received injections of the retrograde tracer CTB (Molecular Probes; 20% solution in 0.1 M PO_4 buffer, pH 7.2). We had previously determined that projections arising from the dentate gyrus and hippocampus in the monkey were ipsilateral, except in their most rostral portion (Amaral et al., 1984). All tracer substances were iontophoretically injected (30–45-minute injections with 5 μAmp DC pulses; 7 seconds on, 7 seconds off) through glass micropipettes (20–30-μm tips). After injection of the tracer, the pipette was withdrawn in three stages to minimize leakage along the pipette tract. First, it was left at the injection site for 1 minute, then raised 100 μm and left there for 5 minutes. Finally, the pipette was slowly withdrawn from the brain at a rate of about 2 mm/minute. Animals survived for 14 days, were deeply anesthetized with sodium pentobarbital (50 mg/kg i.v.; Fatal-Plus; Vortech Pharmaceuticals, Dearborn, MI), and perfused transcardially with ice-cold 1% and 4% paraformaldehyde in 0.1 M phosphate buffer (pH 7.4). The brains were postfixed for 6 hours in the same fixative, cryoprotected in 10% and 20% glycerol solutions in 0.1 M phosphate buffer (pH 7.4; for 24 and 72 hours, respectively), rapidly frozen in isopentane, and stored at –70°C until sectioning. Sections were cut at 30 μm on a freezing, sliding microtome and processed for the visualization of the tracer substances.

Tissue processing

Free-floating sections were processed with constant agitation, at room temperature (unless specified otherwise), for the detection of the transported substance (Lavenex et al., 2004). Immunohistochemistry for PHA-L and CTB was carried out as follows. Sections were rinsed for 3 × 10 minutes in 0.02 M KPBS (pH 7.4), incubated for 15 minutes in 0.5% H_2O_2, washed for 6 × 5 minutes in 0.02 M KPBS, and incubated for 4 hours in a blocking solution made of 0.5% Triton X-100 (TX-100; Fisher Scientific, Fair Lawn, NJ), 5% normal goat serum (NGS; Chemicon, Temecula, CA) in 0.02 M KPBS. Sections were then incubated for 40 hours at 4°C in a solution containing a primary antibody against the tracer substance (rabbit anti-PHA-L at 1:12,000 from Vector Laboratories, rabbit anti-CTB at 1:2,500 from Fitzgerald in 0.3% TX-100, 2% NGS in 0.02 M KPBS). The procedure for visualizing calretinin-positive fibers and cell bodies was carried out on free-floating sections using a mouse anticalretinin monoclonal antibody (SWant, Bellinzona, Switzerland; catalog No.

6B3, lot No. 010399). This antibody was raised in mouse by immunization with recombinant human calretinin-22k. Calretinin-22k is an alternative splice product of the calretinin gene and is identical to calretinin up to Arg178. After fusion, hybridoma cells were screened with human recombinant calretinin as target, the clone 6B3 was selected, and ascites was produced. The antibody 6B3 recognizes an epitope within the first four EF-hands domains common to both calretinin and calretinin-22k. This antibody does not cross-react with calbindin-D28K or other known calcium-binding proteins, as determined by immunoblots (SWant).

After incubation in primary antiserum, sections were washed for 3 × 10 minutes in 0.02 M KPBS containing 2% NGS and incubated for 1 hour in a solution containing a biotinylated secondary antibody against rabbit (goat anti-rabbit IgG at 1:227 from Vector Laboratories in 0.3% TX-100, 2% NGS in 0.02 M KPBS). Sections were rinsed for 3 × 10 minutes in 0.02 M KPBS containing 2% NGS and incubated for 45 minutes in a solution containing an avidin-biotin complex (Biomeda Biostain Super ABC Kit; Biomeda, Foster City, CA; in 0.02 M KPBS). Sections were then rinsed for 3 × 10 minutes in 0.02 M KPBS containing 2% NGS and incubated for another 45 minutes in the solution containing the biotinylated secondary antibody (goat anti-rabbit IgG at 1:227 with 0.3% TX-100, 2% NGS in 0.02 M KPBS). Sections were next rinsed for 3 × 10 minutes in 0.02 M KPBS (with no NGS) and incubated for another 30 minutes in the solution containing the avidin-biotin complex. Sections were then rinsed for 3 × 10 minutes in 50 mM Tris buffer (pH 7.4) and incubated for 45 minutes in a DAB-peroxidase solution containing 0.05% DAB (0.5 mg/ml of 3,3′-diaminobenzidine; Fisher Scientific) and 0.04% H_2O_2 in Tris buffer. Finally, sections were rinsed for 2 × 10 minutes in Tris buffer and for 1 × 10 minutes in 0.02 M KPBS, mounted on gelatin-coated slides, and dried at 37°C overnight. The mounted sections were then processed for intensification of the DAB reaction product. Sections were defatted for 2 × 2 hours in a mixture of ethanol-chloroform (50:50, v/v), hydrated through a graded series of ethanol solutions (2 minutes each in 100%, 100%, 95%, 70%, 50% EtOH), and rinsed in running dH_2O for 10 minutes. Sections were incubated for 40 minutes in a 1% silver nitrate solution at 56°C (protected from light) and rinsed in running dH_2O for 10 minutes (protected from light). Sections were then incubated for 10 minutes in 0.2% gold chloride at room temperature and rinsed in running dH_2O for 10 minutes (protected from light). Sections were stabilized in 5% sodium thiosulfate at room temperature for 15 minutes (protected from light) and rinsed in running dH_2O for 10 minutes. Finally, sections were dehydrated through a graded series of ethanol solutions (4 minutes each in 50%, 70%, 95%, 100%, 100% EtOH) and cleared with xylene (3 × 4 minutes in 100% xylene) and the slides coverslipped with DPX (BDH Laboratory Supplies, Poole, United Kingdom).

BDA processing was as follows. Sections were rinsed for 3 × 10 minutes in 0.02 M KPBS, incubated for 15 minutes in 0.5% H_2O_2, washed for 6 × 5 minutes in 0.02 M KPBS, and incubated for 1 hour in a solution comprised of 1% Triton X-100 (TX-100; Fisher Scientific) in 0.02 M KPBS. Sections were then incubated overnight at 4°C in a solution made up of an avidin-biotin complex (Biomeda Biostain Super ABC Kit), with 0.3% TX-100 in 0.02 M KPBS. Sections were rinsed for 3 × 10 minutes in 50 mM Tris buffer and incubated for 45 minutes in a DAB-peroxidase solution containing 0.05% DAB, 0.015% H_2O_2 in Tris buffer. Sections were then rinsed for 2 × 10 minutes in Tris buffer and for 1 × 10 minutes in 0.02 M KPBS, mounted on gelatin-coated slides, and placed to dry at 37°C overnight. The mounted sections were then processed for intensification of the DAB reaction product and coverslipped as described previously.

Data analysis

The distribution of anterogradely labeled fibers through the entire rostrocaudal extent of the dentate gyrus and hippocampus was analyzed using darkfield optics. To represent the gradients of fiber termination in the dentate gyrus and CA3, low-magnification photomicrographs were taken of representative sections for each case. Photomicrographs were taken with a Leitz DMRD microscope. Plotting of retrogradely labeled cells for CTB was done using the Neurolucida computer-aided microscope system (MicroBrightField, Colchester, VT). We estimated the lengths of the mossy fibers, associational projection, and local projections along the rostrocaudal axis by multiplying the number of coronal sections in which labeling was observed by the distance between sections. We measured the length of the mossy fibers at the level of the genu of the hippocampus on two-dimensional reconstructions of fiber trajectories. To describe the locations of the injection sites more precisely, we calculated the ratio of the distance from the rostral edge of the dentate gyrus to the center of the injection site divided by the full rostrocaudal distance of the dentate gyrus. An AP ratio less than 0.33 indicates an injection site located in the rostral one-third of the dentate gyrus. An AP ratio between 0.33 and 0.66 indicates an injection site located in the middle one-third, whereas an AP ratio larger than 0.66 indicates an injection site located in the caudal one-third of the dentate gyrus.

RESULTS

Cytoarchitecture of the dentate gyrus

The nomenclature and cytoarchitectonic subdivisions of the monkey hippocampal formation have been described previously (Amaral et al., 1984; Pitkanen and Amaral, 1993; Amaral and Lavenex, 2007). The major subdivisions of the monkey hippocampal formation are indicated in a representative Nissl-stained coronal section at a midrostrocaudal level in Figure 1.

The dentate gyrus comprises three layers: a cell-dense granule cell layer, a relatively cell-free molecular layer that lies superficial to the granule cell layer and is bounded by the hippocampal fissure or ventricle, and a narrow polymorphic layer located subjacent to the granule cell layer (Fig. 2). In monkeys, it is difficult to differentiate the diffusely organized cells of the polymorphic layer from the nearly as diffuse hilar portion of the CA3 field of the hippocampus in Nissl-stained preparations (Fig. 2A). Calretinin immunoreactivity is an excellent marker of the polymorphic layer and distinguishes it from the proximal portion of the CA3 field (Fig. 2B). We use the term *rostrocaudal axis* to refer to the longitudinal axis of the hippocampal formation. The axis orthogonal to the rostrocaudal axis is called the *transverse axis*. The portion of CA3 located closest to the dentate gyrus is called *proximal* and

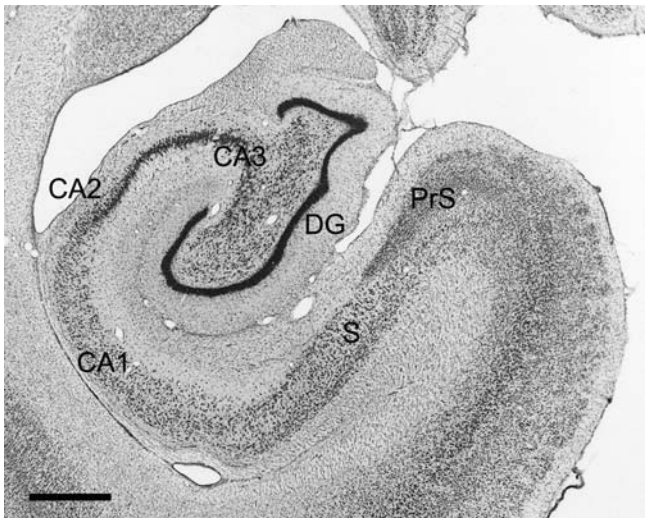

Fig. 1. Brightfield photomicrograph of a Nissl-stained coronal section at midrostrocaudal level through the *Macaca fascicularis* monkey hippocampal formation, illustrating the position of the dentate gyrus relative to the other fields of the hippocampal formation. DG, dentate gyrus; CA3, CA2, CA1, fields of the hippocampus; S, subiculum; PrS, presubiculum. Scale bar = 1 mm.

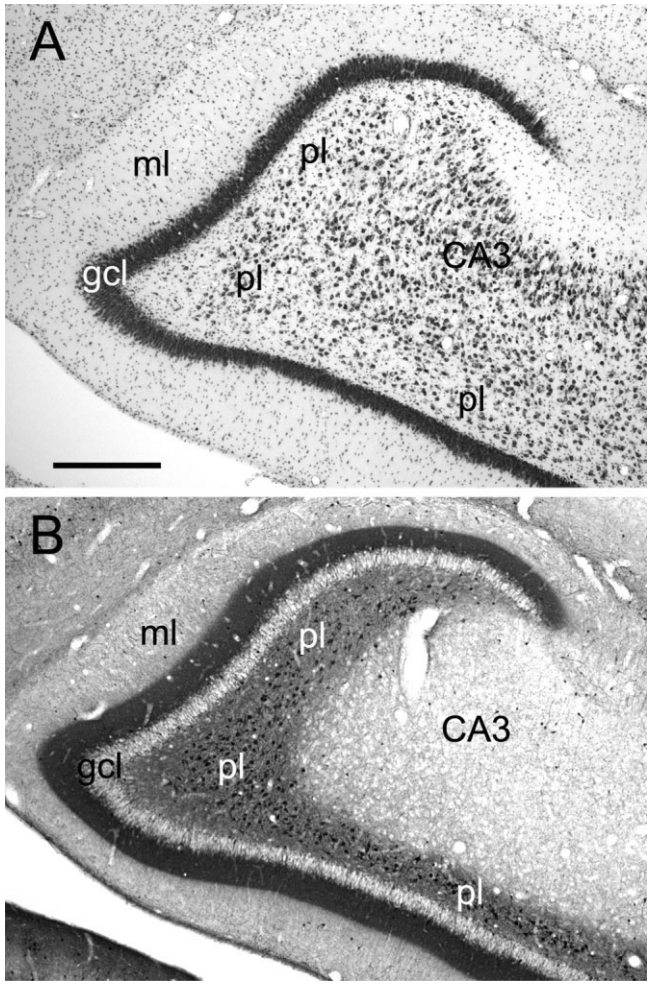

Fig. 2. Photomicrographs of a coronal section through the rostral portion of the *Macaca fascicularis* monkey dentate gyrus. **A:** Nissl-stained section. **B:** Adjacent section stained for calretinin immunoreactivity. The dentate gyrus comprises three layers, including the molecular layer (ml), the granule cell layer (gcl), and the polymorphic layer (pl) or hilus. Note that calretinin immunoreactivity is dense in the polymorphic layer and thus helps define the boundary with the CA3 field of the hippocampus. Calretinin staining is also dense in the inner one-third of the molecular layer, where the associational projections terminate. Scale bar = 0.5 mm.

that closer to CA2 is called *distal*. We use the term *superficial* to mean toward the hippocampal fissure or ventricle and the term *deep* to indicate the opposite direction (Amaral and Lavenex, 2007).

We call the most medial portion of the rostral hippocampal formation the *uncus* or *uncal portion*. The flexed, rostrally located portion that runs mediolaterally is called the *genu*, and the laterally situated, main portion of the hippocampus is called the *body*. We refer to the portion of the dentate gyrus that lies adjacent to the hippocampal fissure as the *suprapyramidal blade* and the opposite blade as the *infrapyramidal blade*; the connecting portion is referred to as the *crest*.

Description of the injection sites

Figure 3 presents the maximal extent of the 20 anterograde tracer injections analyzed in this study. Regardless of whether the injection was on the left or right side of the brain, it is depicted on sections drawn from the left dentate gyrus.

Seven anterograde tracer injections involved the uncus, genu, and the rostral one-third of the body of the hippocampus. In most cases, the injection involved all layers of the dentate gyrus. M-13-92 (PHA-L) involved the molecular layer of the dentate gyrus as well as CA1. M-03-02-L (PHA-L) was located in the molecular layer and also involved the adjacent stratum lacunosum-moleculare of CA3. M-03-02-R (BDA) was located medially in the uncal portion of the dentate gyrus. This was the most "rostral" injection into the dentate gyrus. M-02-02 (PHA-L) was located at the transition between the genu and the rostral body of the dentate gyrus. M-05-92 (PHA-L) was located in the suprapyramidal blade of the dentate gyrus. This injection also involved the distal dendrites of CA1 pyramidal neurons in the stratum lacunosum-moleculare. M-12-92 (PHA-L) was confined to the suprapyramidal blade of the dentate gyrus. M-11-92 (PHA-L) also involved the suprapyramidal blade.

There were nine anterograde tracer injections that involved the midrostrocaudal one-third of the dentate gyrus. M-09-93 (BDA) was located in the infrapyramidal blade of the dentate gyrus. The injection also involved the hilar portion of CA3. M-11-92-R (PHA-L) was at the tip of the suprapyramidal blade of the dentate gyrus and involved the superficial layers of proximal CA3 and strata radiatum and lacunosum-moleculare. M-10-93 (BDA) involved the crest of the dentate gyrus and underlying hilar CA3. M-01-92 (PHA-L) involved the crest of the dentate gyrus. M-09-92 (PHA-L) also involved the crest of the dentate gyrus. M-27-92 (PHA-L) involved the tip of the suprapyramidal blade of the dentate gyrus, as did M-09-03-L (PHA-L). M-02-92 (PHA-L) was slightly caudal to the pre-

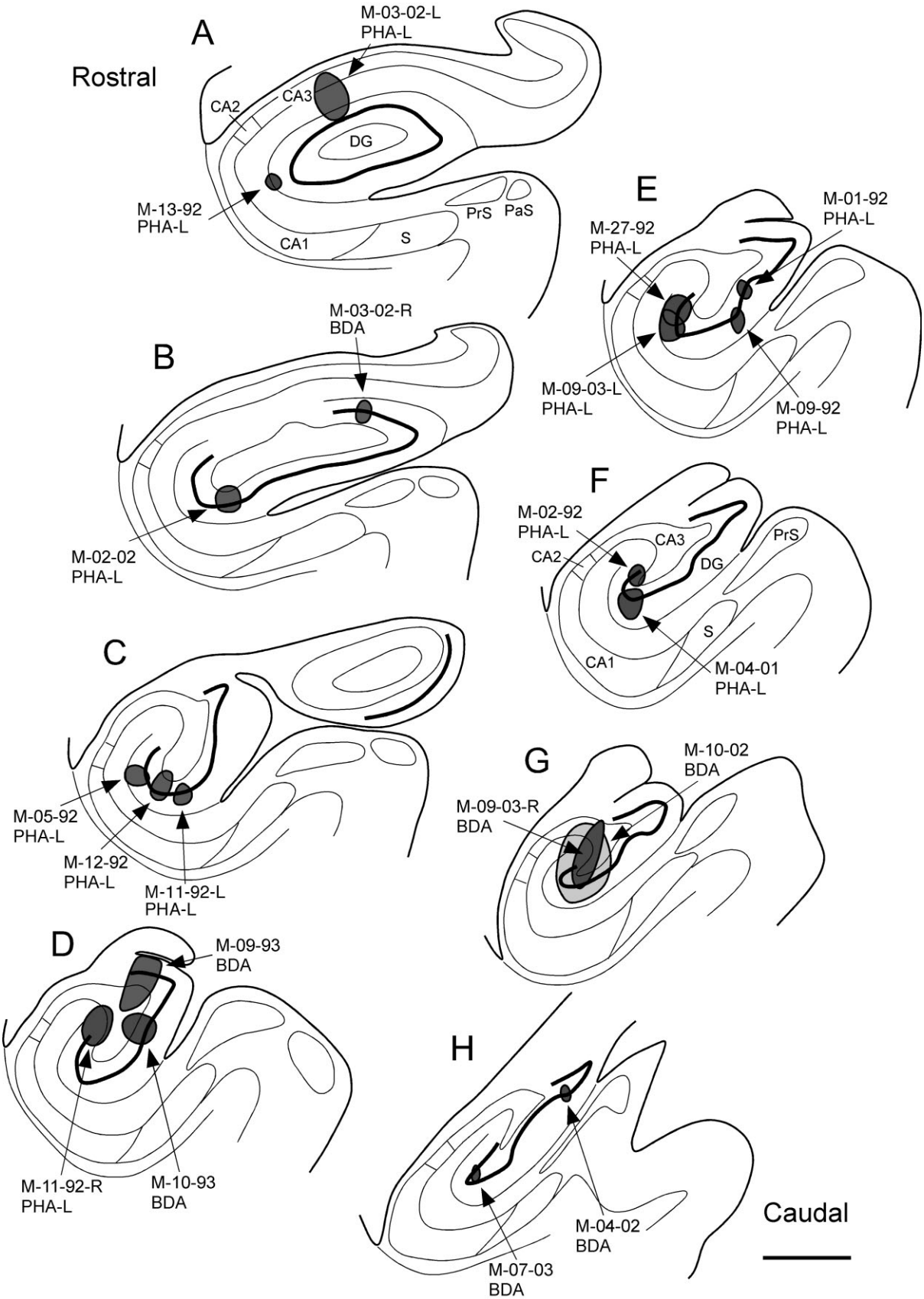

Fig. 3. **A–H:** Series of line drawings of coronal sections through the monkey hippocampal formation arranged from rostral (A) to caudal (H). The locations and approximate sizes of the central portions of anterograde tracer injections analyzed in this study are plotted at appropriate levels. Injection sites in both left and right hemispheres are plotted on sections of the left hemisphere. Scale bar = 1 mm.

vious two injections but also involved the suprapyramidal blade of the dentate gyrus and the pyramidal cell layer and the stratum radiatum of proximal CA3. M-04-01 (PHA-L) was also confined to the suprapyramidal blade of the dentate gyrus.

There were four anterograde tracer injections in the caudal one-third of the dentate gyrus. M-09-03-R (BDA) involved the suprapyramidal blade of the dentate gyrus and the stratum radiatum and pyramidal cell layer of CA3. M-10-02 (BDA) was quite large and involved the suprapyramidal blade of the dentate gyrus, strata radiatum and lacunosum-moleculare, and pyramidal cell layer of CA3. M-07-03 (BDA) involved the suprapyramidal blade of the dentate gyrus. M-04-02 (BDA) was at the same level as M-07-03 but involved the infrapyramidal blade of the dentate gyrus.

In addition to the anterograde tracer injections, there were also five cases in which the retrograde tracer CTB was injected. These injections involved the dentate gyrus at various rostrocaudal levels. These experiments were analyzed to identify the cell bodies of origin for the various projections that we discuss.

Mossy fibers

The morphology of the monkey mossy fibers (Fig. 4) appeared similar to that seen in rats (Claiborne et al., 1986). The main mossy fiber axon had a diameter of approximately 0.6 μm. Large "mossy fiber expansions" were periodically seen along the length of the mossy fibers. These presynaptic profiles were irregularly shaped and varied in size, but the larger of the expansions were on the order of 3–5 μm in cross-sectional diameter. These large expansions gave rise to several filipodial extensions that also had varicosities along their extents (Fig. 4B). The mossy fibers also gave rise to thinner collaterals that either had spherical varicosities or terminated with a small mossy fiber expansion and produced a dense plexus within the polymorphic layer of the dentate gyrus.

The general pattern of mossy fiber projections was consistent across all experimental cases. The mossy fibers traveled mainly within the CA3 pyramidal cell layer (Fig. 5), with a slight rostral inclination (Figs. 6, 7). Axons of the mossy fibers extended throughout the full transverse extent of the CA3 field (Fig. 5). Once the mossy fibers reached the distal portion of CA3, they changed direction and extended toward the rostral pole of the hippocampus (Figs. 6, 7). The fibers took this course in the stratum lucidum just superficial to the CA3 pyramidal cell layer in what has been called the "end bulb" in nonprimate species (Amaral and Lavenex, 2007). Regardless of the rostrocaudal or transverse location of the injection sites, the mossy fibers were found to travel for 3–5 mm rostrally (Table 1).

Case M-04-01 (Fig. 6) is representative of injections at midrostrocaudal level of the dentate gyrus (Fig. 3D–F). In this case, labeled mossy fibers were distributed in the polymorphic layer (Fig. 6E) and continued transversely within the pyramidal cell layer to the distal tip of CA3 (Fig. 6D,E). The transversely oriented bundles of labeled mossy fibers were about 2.7 mm in length (Table 1). The mossy fibers appeared to be completely interdigitated with the CA3 pyramidal cells that form the most proximal or hilar portion of the CA3 region. As the fibers exited the hilar region, they were located below, within, and above the pyramidal cell layer (Figs. 5, 6D). There were no clearly defined suprapyramidal, intrapyramidal, and infrapyramidal bundles as in the rodent brain. Fibers that were initially located deep to the pyramidal cell layer ascended through the pyramidal cell layer and traveled to the distal portion of CA3 in a position superficial to the pyramidal cell layer. After the fibers completed their transverse trajectory, they turned and continued in the end bulb region (Fig. 6B,C), where they extended rostrally for 5.3 mm, or approximately 40% of the full rostrocaudal extent of the hippocampus. It is important to point out that mossy fiber expansions were evident on the fibers through the entire rostrocaudal extent of the end bulb projection. This would suggest that these mossy fibers formed synapses with pyramidal neurons located in the distal portion of CA3. In other words, although pyramidal cells through the full transverse extent of the CA3 layer are potentially capable of receiving input from granule cells located at the same level, distally located pyramidal cells could receive mossy fiber termination arising from granule cells located as far as 3–5 mm caudally.

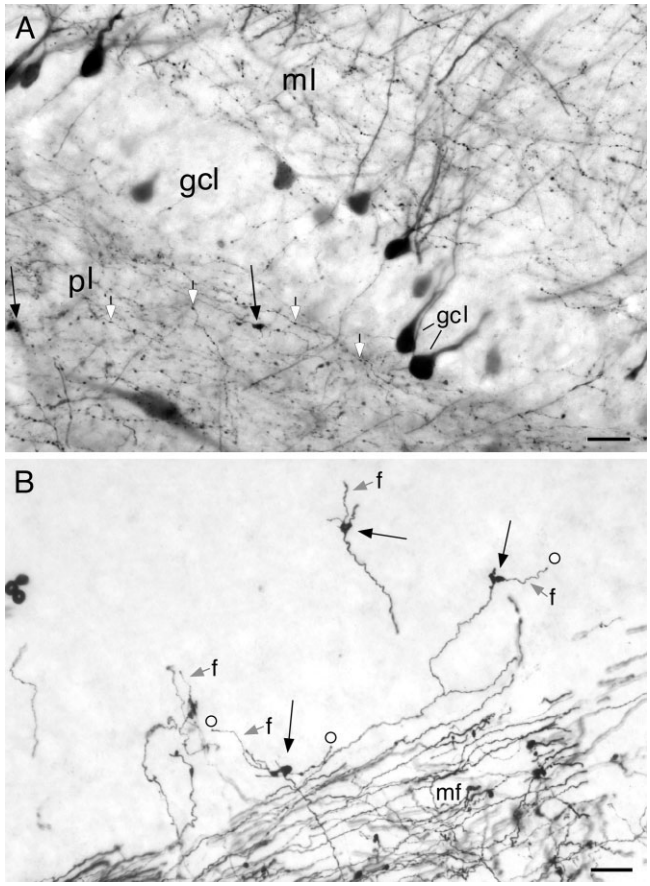

Fig. 4. Photomicrographs of PHA-L labeled mossy fibers. **A:** Granule cells and mossy fibers traveling within the polymorphic layer of the dentate gyrus. There are small versions of the mossy fibers expansions (black arrows) as well as more numerous en passant, spherical varicosities (white arrows). **B:** Photomicrographic montage of PHA-L labeled mossy fibers (mf) in the CA3 region of the hippocampus. Several isolated mossy fiber expansions (black arrows) are illustrated. These typically have several long filipodial extensions (gray arrows, f) that generally terminate with a spherical ending (circle). Scale bars = 20 μm.

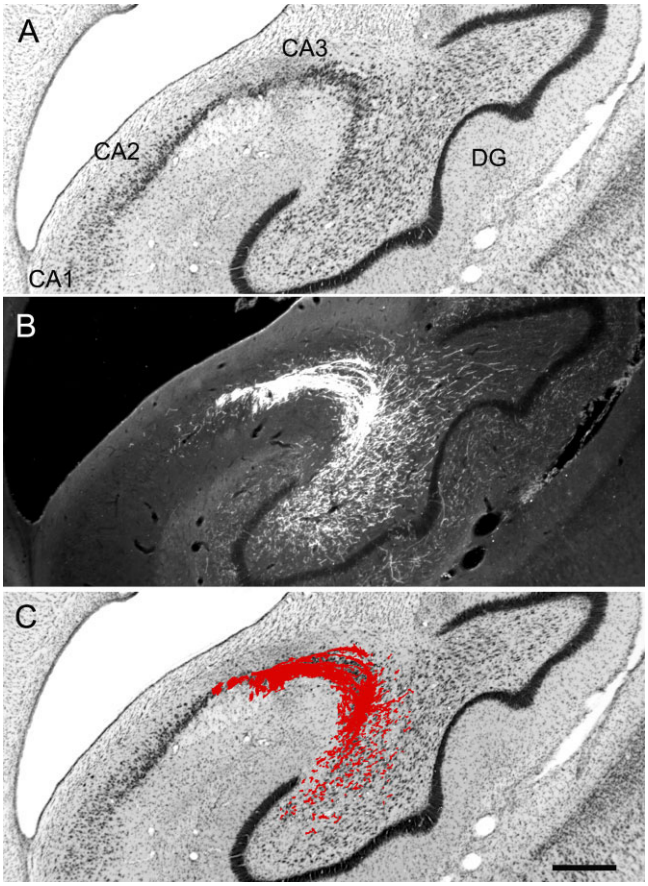

Fig. 5. Overview of the transverse trajectory of mossy fibers. **A:** Nissl-stained coronal section of the dentate gyrus and CA3 field of the hippocampus. **B:** Darkfield photomicrograph of a section adjacent to the one in A showing PHA-L-labeled mossy fibers (case M-04-01) as they traverse the CA3 field of the hippocampus. This section is 0.7 mm rostral to the injection site. **C:** Superimposition of the mossy fiber labeling onto the Nissl-stained section. This illustrates that the mossy fibers travel deep to, within, and superficial to the pyramidal cell layer. Scale bar = 0.5 mm.

Mossy fibers also gave rise to collaterals that innervated the polymorphic layer of the dentate gyrus. As illustrated in Figure 6E, these collaterals had a very limited spatial distribution. With this suprapyramidally placed injection, polymorphic layer collaterals were mainly limited to the suprapyramidal tip of the dentate gyrus, although very weak labeling was also observed outside of the suprapyramidal region. These collaterals were seen only at the levels at which the mossy fibers have a transverse orientation (i.e., for about 0.7 mm). Axons within the polymorphic layer had either large mossy fiber expansions or smaller, spherical varicosities (Fig. 4).

The pattern of projections observed in case M-04-01 was also observed in case M-10-93, which had a BDA injection at a midrostrocaudal level (Fig. 7E). The distribution of the mossy fibers to the polymorphic layer was more widespread in this case, such that axon collaterals terminated throughout the entire transverse extent of the dentate gyrus (Fig. 7D,E). Note again the prominent collection of transversely oriented fibers in CA3 (Fig. 7D, small arrow) and the rostrocaudally oriented fibers in the end bulb region (Fig. 7B,C, small arrows). For cases with injections at these levels, the rostrocaudal length of the mossy fibers ranged from 2.6 to 5.7 mm (Table 1), which on average represented approximately 30% of the total rostrocaudal length of the hippocampus.

A similar pattern of mossy fiber projections was observed when the injection involved rostral levels of the dentate gyrus (Fig. 3A–C). The injection in M-13-92 was located in the lateral aspect of the genu (Fig. 8B). The rostrocaudal component is oriented primarily in the coronal plane (Fig. 8A). In the cases with injections at rostral levels, the longitudinal distance of the mossy fibers ranged from 2.3 to 3.7 mm (Table 1). We had a number of injections located at caudal levels of the dentate gyrus (Fig. 3G,H), and again the basic pattern of projections was very similar to the more rostrally placed injections. In case M-07-03, the injection was located in the suprapyramidal blade (Fig. 9E). The mossy fibers terminated mainly subjacent to the injection, but very weak labeling was present throughout much of the rest of the polymorphic layer (Fig. 9D,E). Labeled mossy fibers extended for approximately 3.6 mm in the rostral direction (Fig. 9A,B). The length of the mossy fibers along the long axis for these caudal injections ranged from 2.9 to 4.1 mm (Table 1), which is approximately 26% of the total rostrocaudal length of the hippocampus.

Associational projections

In all injections that had some involvement of the polymorphic layer, we observed labeling of the associational projection to the inner one-third of the molecular layer (Fig. 10). Irrespective of the rostrocaudal location of the injection, the associational projection extended for a substantial portion of the longitudinal extent of the dentate gyrus, both rostrally and caudally from the level of the injection. The caudally directed projection was more extensive and substantial than the rostrally directed component of the projection.

The injection in case M-10-93 was located at a midrostrocaudal level of the dentate gyrus (Fig. 3D). In addition to a patch of heavily labeled dentate granule cells, the injection site also involved cells located in the polymorphic layer (Fig. 7). The associational projection was weak or absent at the level of the injection site. However, labeled fibers were observed in the inner one-third of the molecular layer, outside the injection site at more medial or lateral positions of the same coronal section (Figs. 7E, 13B,C). The associational projection extended, from the injection site, for approximately 5.0 mm rostrally and 7.0 mm caudally (Table 2). Significant labeling was thus observed throughout 82% of the full rostrocaudal extent of the dentate gyrus. Fiber and terminal labeling was denser at caudal levels (Figs. 7F,G, 13D) than at levels rostral to the injection (Figs. 7B–D, 13A). As the terminal field became denser at levels away from the injection site, it was also observed throughout the full transverse extent of the dentate gyrus. Although there was a progressive increase in the density of labeling as one progressed away, either rostrally or caudally, from the injection site, the density of labeling fell off at the rostral and caudal extremes of the projection zone (Fig. 7A,H). Case M-04-01, with an injection at approximately the same rostrocaudal level as case M-10-93, demonstrated a similar pattern of projections (Fig. 6). For injections at midrostrocaudal levels, the total

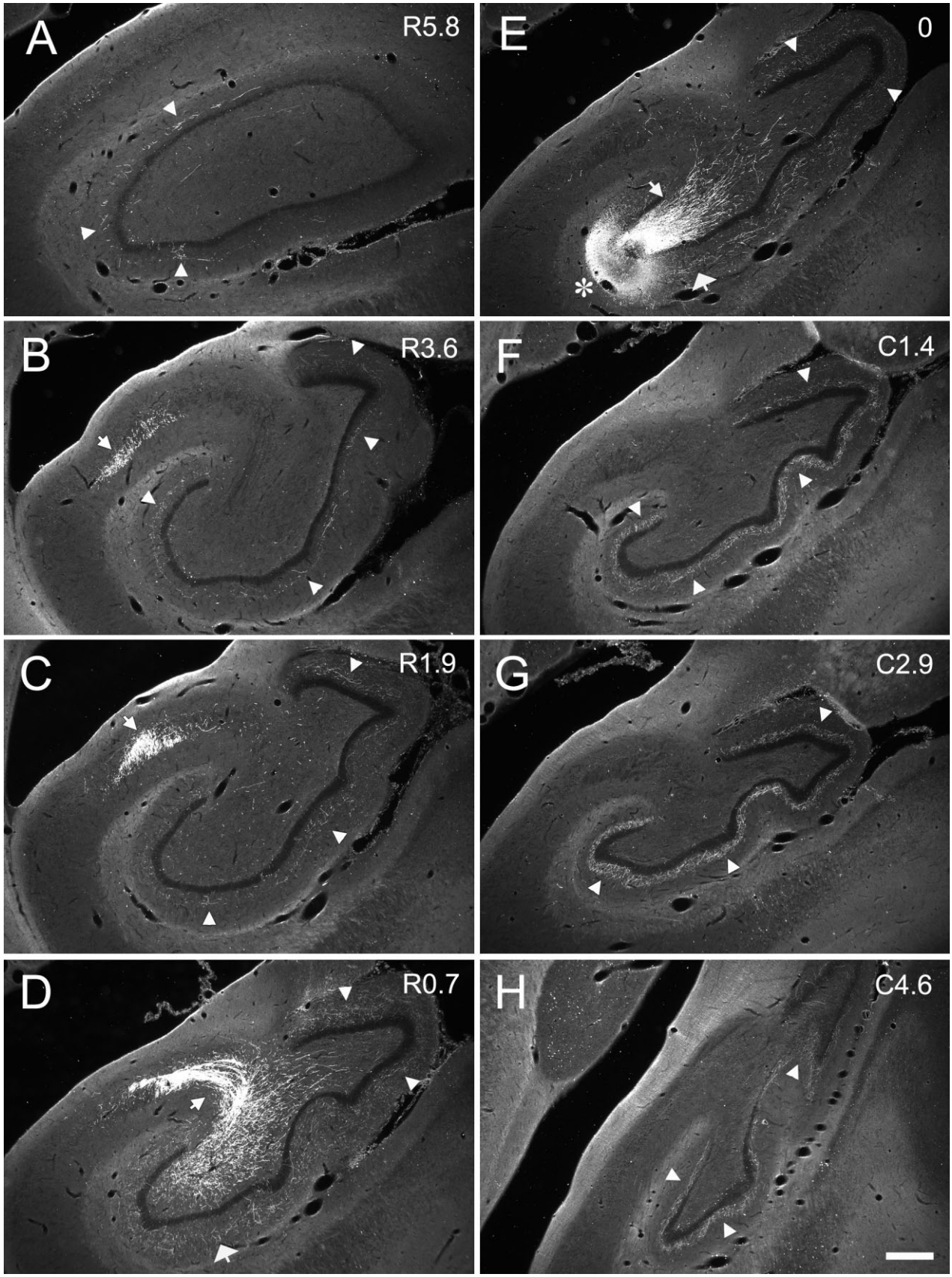

Fig. 6. **A–H:** Darkfield photomicrographs of coronal sections of the dentate gyrus arranged from rostral (A) to caudal (H) showing the distribution of PHA-L-labeled fibers and terminals in case M-04-01. The injection was located in the midrostrocaudal one-third of the dentate gyrus (asterisk in E). The numbers to the right of each panel indicate the distance, in millimeters, of the photographed section from the injection site (R and C indicate rostral and caudal to the injection site, respectively). Mossy fibers projected transversely to the CA3 field (narrow arrows in D,E) and, at the distal portion of CA3, changed direction and traveled rostrally for several millimeters (narrow arrow in B,C). The associational projection terminated in the inner one-third of the molecular layer (arrowheads) both rostral and caudal to the level of the injection. The projection was densest at levels located caudal to the injection site (F–H) compared with levels located rostrally (C, B, A). Local projections terminated in the outer two-thirds of the molecular layer at the level of injection site (wide arrow in E). Scale bar = 0.5 mm.

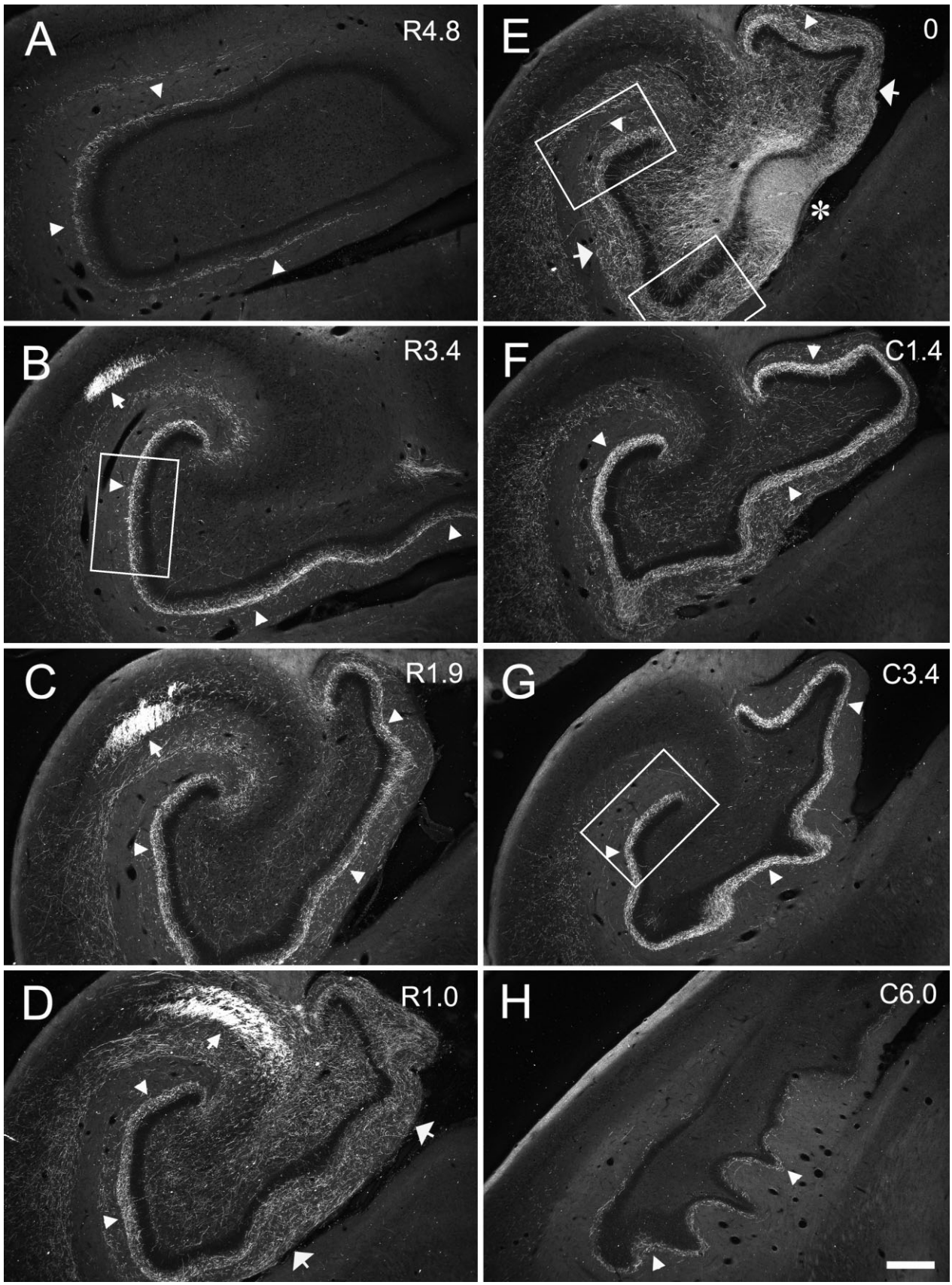

Fig. 7. **A–H:** Darkfield photomicrographs of coronal sections of the dentate gyrus arranged from rostral (A) to caudal (H) showing the distribution of BDA-labeled fibers and terminals in case M-10-93. The injection was located in the midrostrocaudal portion of the dentate gyrus (asterisk in E). Rectangles in E indicate the regions taken for high magnification photomicrographs in Figure 13 (top rectangle corresponding to Fig. 13C and bottom one to Fig. 13B). Note that the mossy fibers travel transversely in the CA3 pyramidal cell layer (D) and then turn rostrally at the distal portion of CA3 (B,C). The associational projection terminates widely both rostrally and caudally to the level of the injection (arrowheads). Local projections are indicated by arrows. Scale bar = 0.5 mm.

TABLE 1. Length of the Transverse and Rostrocaudal Components of the Mossy Fibers

Case	AP ratio	Transverse length (mm)	Rostrocaudal length (mm)	
Rostral				
M1392	0.14	NA	3.5	3.1 (Average)
M0302-L	0.15	NA	3.7	3.5 (Median)
M0302-R	0.17	NA	2.3	0.7 (SD)
M0202	0.20	NA	2.4	
M1192-L	0.29	2.5	3.6	
Middle				
M1292	0.33	3.4	2.9	4.2 (Average)
M1192-R	0.33	2.1	3.5	4.8 (Median)
M0592	0.35	2.4	5.2	1.1 (SD)
M2792	0.44	1.8	5.7	
M0992	0.44	2.2	3.4	
M0903	0.45	1.9	4.8	
M0192	0.45	2.2	2.6	
M0292	0.55	2	4.8	
M0401	0.56	2.7	5.3	
Caudal				
M0903	0.77	1.5	3.8	3.6 (Average)
M1002	0.80	NA	4.1	3.7 (Median)
M0703	0.89	2.4	3.6	0.5 (SD)
M0402	0.91	1.5	2.9	

distance of the associational projection ranged from 10.6 to 12.0 mm (Table 2), or approximately 80% of the total length of the dentate gyrus.

Labeling of the associational projection at any particular rostrocaudal level was rather homogeneous throughout the full transverse extent of the dentate gyrus except at the level of the injection site. Labeling was not uniformly distributed, however, in the inner one-third of the molecular layer. This can be seen in the higher magnification photomicrographs from case M-10-93 (Fig. 13). Particularly at levels far rostral from the injection site (Fig. 13A), there was a gap just superficial to the granule cell layer that was devoid of associational projections. At these levels, the labeled terminals were densest in the outer part of the inner one-third of the molecular layer (Figs. 7A,B, 13A).

We observed a very similar pattern of the associational projection arising from the rostral one-third of the dentate gyrus (Fig. 3A–C). In case M-02-02 (Fig. 11), the PHA-L injection revealed an associational projection that extended as far as the rostral end of the dentate gyrus (Fig. 11A,B) to very nearly the caudal pole (Fig. 11H). In this case, the associational projection extended for approximately 13 mm rostrocaudally (Table 2), or 84% of the full rostrocaudal length of the dentate gyrus. This case also demonstrated the radial differences in the terminal field at rostral or caudal levels from the injection site. As one proceeded rostrally (Fig. 11A,B), the terminal zone left a gap above the granule cell layer that widened further at more rostral levels. At levels caudal to the injection, there was no gap above the granule cell layer, and, in contrast to what was observed rostrally, the outer portion of the inner one-third of the molecular layer became devoid of associational projections at caudal levels.

The associational projection arising from caudal levels of the dentate gyrus (Fig. 3G,H) tended to be somewhat more limited. In case M-09-03 (Fig. 12), the BDA injection revealed associational projections that extended for approximately 3.8 mm rostrally and 2.2 mm caudally, which is approximately 44% of the full rostrocaudal length of the dentate gyrus. On average, the full length of the associational projection arising from caudal levels was approximately 6.3 mm (Table 2), or about 45% of the length of the dentate gyrus.

Organization of the local projections

In addition to the mossy fibers and the associational projection, local projections were observed in all cases in which the injection involved cells of the polymorphic layer. Local projections were observed to the outer two-thirds of the molecular layer; they were most dense at the level of the injection site. The local projections, however, extended well beyond the level of the injection site, although they were never as extensive as the associational projection to the inner molecular layer. For the quantitative data described below, we considered the projection to be present even if only a few fibers were observed in the outer two-thirds of the molecular layer. It should be noted, however, that the density of fiber and terminal labeling tended to drop off quite rapidly as one proceeded away from the level of the injection site.

In case M-10-93, the BDA injection revealed substantial local projections to the outer two-thirds of the molecular layer (Figs. 7, 13B). Unlike the associational projection, the density of labeled fibers and terminals decreased as one moved either rostrally or caudally from the level of the injection (Figs. 7, 13). In this case, the local projections extended for approximately 4.1 mm rostrally and 3.8 mm caudally (Table 3), which is approximately 54% of the rostrocaudal length of the dentate gyrus. The rostrocaudal extent of local projections in cases with injections at midrostrocaudal levels ranged from 3.1 to 7.9 mm (mean = 5.5 mm), or approximately 40% of the full rostrocaudal extent of the dentate gyrus.

Similar results were obtained in cases with rostral and caudal injections (Fig. 3A–C,G–H). In case M-02-02 located rostrally (Fig. 11), local projections to the outer two-thirds of the molecular layer extended for approximately 8.9 mm rostrocaudally (Table 3), or approximately 58% of the length of the dentate gyrus. In case M-09-03 located caudally (Fig. 12), the local projections extended for approximately 3.6 mm rostrally and 2.2 mm caudally, or approximately 42% of the full rostrocaudal extent of the dentate gyrus (Table 3).

Retrograde tracer injections in the dentate gyrus

We placed five CTB injections into the dentate gyrus to confirm the topographical organization of the cells of origin of the associational projection in the dentate gyrus. The CTB injection in case M-04-02-L involved all layers of the suprapyramidal blade of the dentate gyrus (Fig. 14A). The injection also involved the subjacent portion of the hilar CA3 region. For the purposes of this paper, we only plotted the distribution of retrogradely labeled cells in the polymorphic layer of the dentate gyrus (Fig. 15). The labeled cells were distributed very widely along the rostrocaudal axis but were more substantial in sections located rostrally than caudally to the injection (Figs. 15).

DISCUSSION

The aim of this study was to determine the topographical organization of the major connections of the macaque monkey dentate gyrus, namely, the mossy fibers, the associational projection, and the local projections. The main findings, summarized in Figures 16 and 17, are as follows.

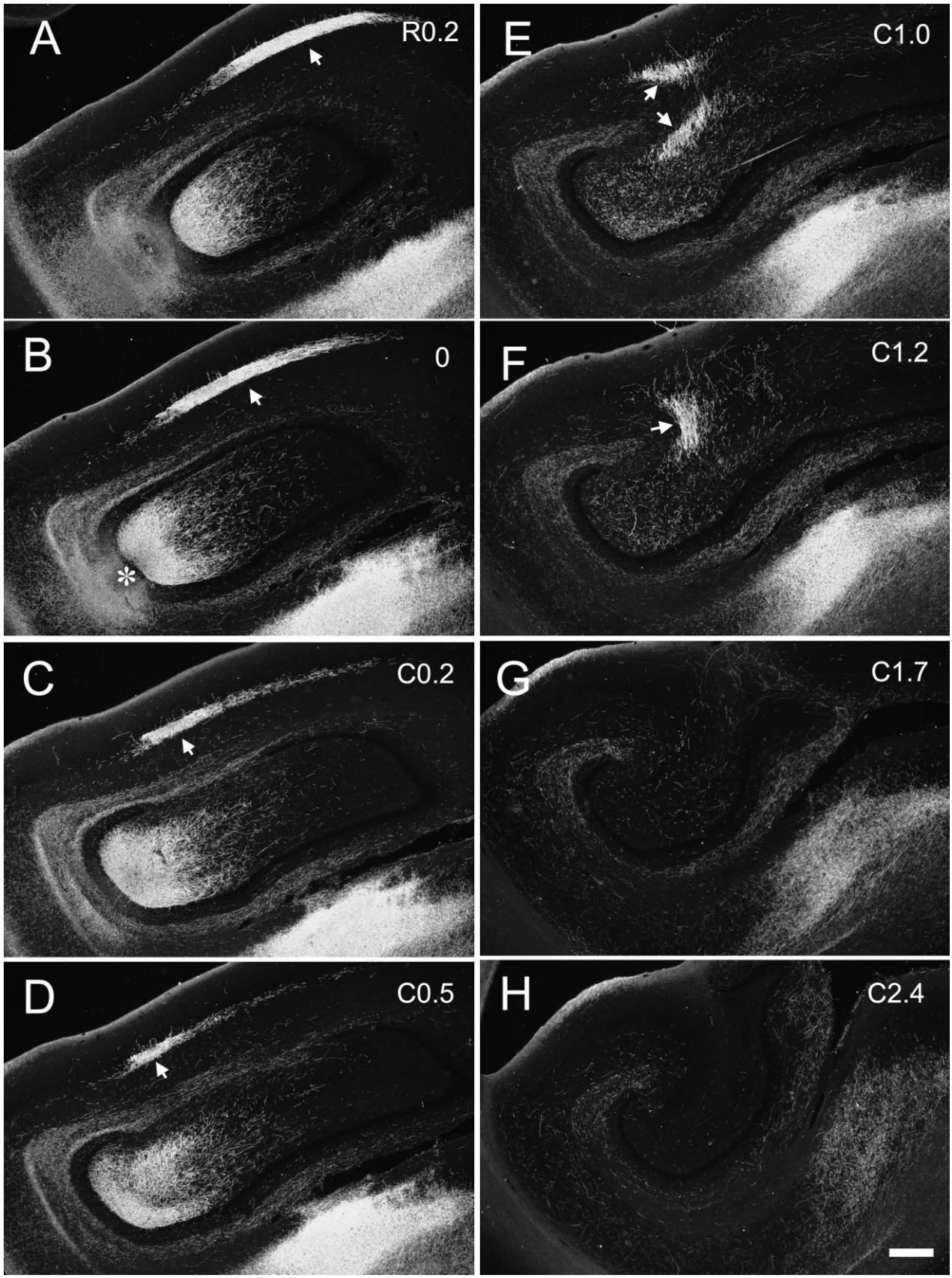

Fig. 8. **A–H:** Darkfield photomicrographs of coronal sections of the dentate gyrus arranged from rostral (A) to caudal (H) showing the distribution of PHA-L-labeled fibers and terminals in case M-13-92. The injection was located in the rostral portion of the dentate gyrus at the level of the genu (asterisk in B). Note that the mossy fibers are distributed through the full transverse extent of CA3 (E,F). At the distal portion of CA3, the mossy fibers travel medially toward the uncus, which corresponds to the rostrally oriented projection (A–D). Because the hippocampus curves medially (white arrows) at this level, the transverse component of the mossy fiber appears in the sections caudal to the injection and the longitudinal component appears to travel parallel to the coronal plane. Scale bar = 0.5 mm.

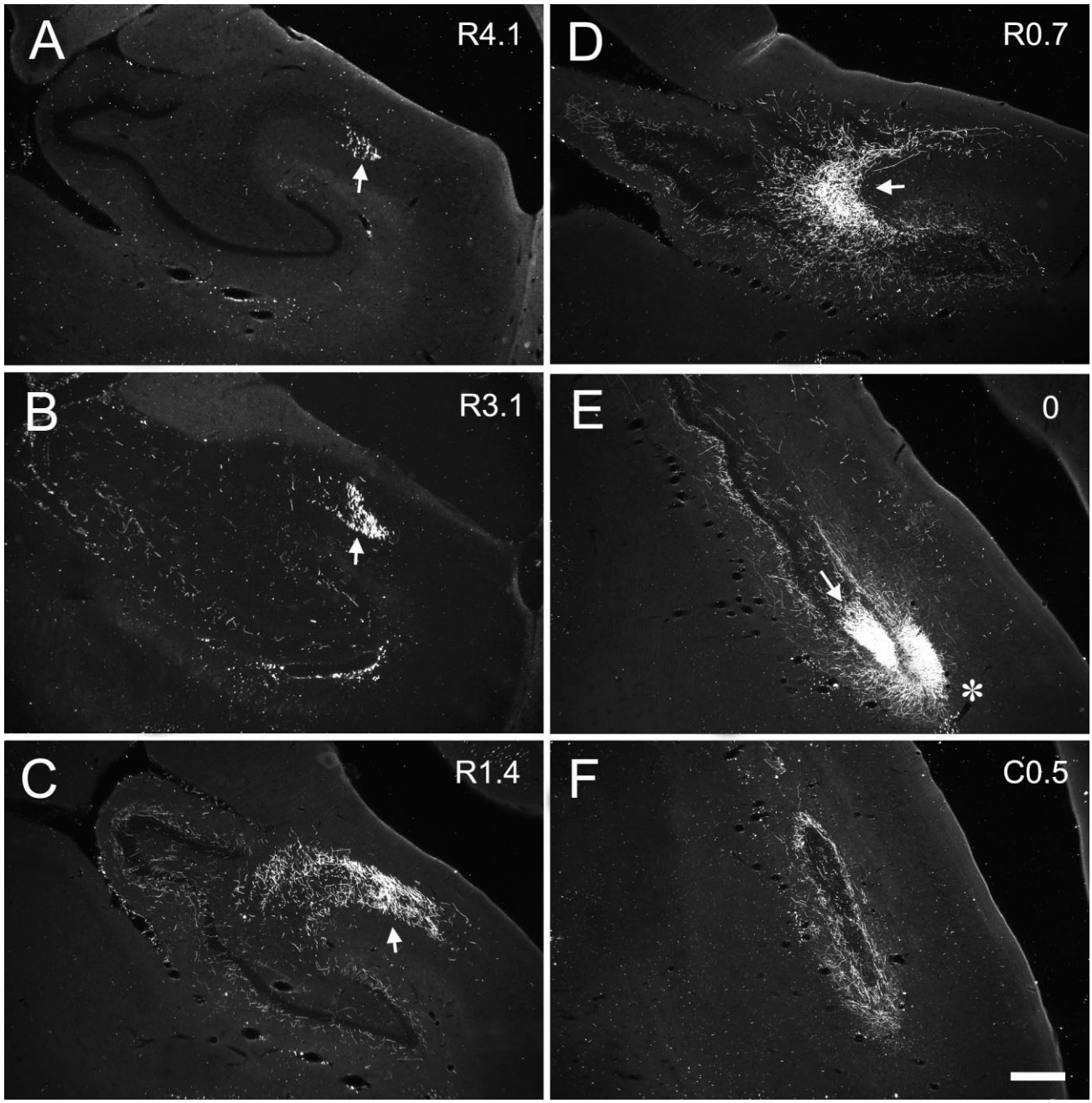

Fig. 9. **A–F:** Darkfield photomicrographs of coronal sections of the dentate gyrus arranged from rostral (A) to caudal (F) showing the distribution of PHA-L-labeled fibers and terminals in case M-07-03. The injection is located in the caudal one-third of the dentate gyrus (asterisk in E). Note that the mossy fibers travel throughout the entire transverse extent of CA3 (C–E) and travel rostrally at the end bulb region of distal CA3 (B). Scale bar = 0.5 mm.

The granule cells give rise to mossy fibers that terminate on a number of neuronal types both within the polymorphic layer of the dentate gyrus and within the CA3 field of the hippocampus. The mossy fibers travel throughout most of the transverse extent of CA3 at approximately the same rostrocaudal level as the cells of origin but with a slight rostral inclination. Once the mossy fibers reach the distal portion of CA3, they change course and travel rostrally for 3–5 mm, or about 30% of the length of the hippocampus.

Mossy cells in the polymorphic layer give rise to the associational projection, which terminates in the inner one-third of the molecular layer and extends widely both rostrally and caudally from the cells of origin. The associational projection is very meager at the level of the injection site, except at a distance away from the injection

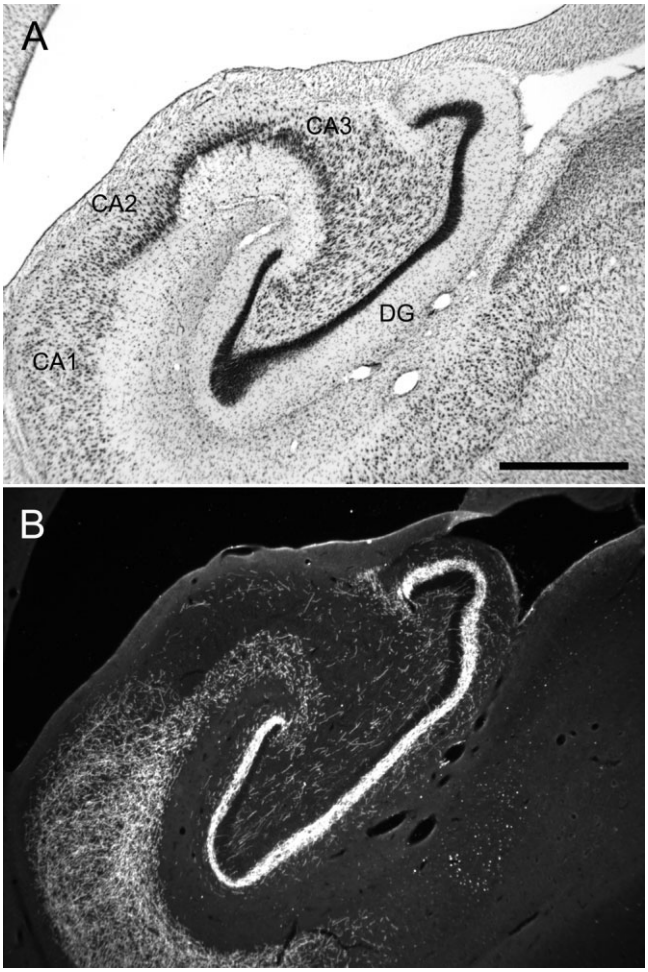

Fig. 10. Overview of the associational projections. **A:** Nissl-stained coronal section of the dentate gyrus and hippocampus. **B:** Darkfield photomicrograph of a section adjacent to the one in A showing PHA-L-labeled associational projections (case M-02-02). This section is 3.4 mm caudal to the injection site. Note that the associational projection terminates in the inner one-third of the molecular layer of the dentate gyrus. The strong projection is present throughout the entire transverse extent of the dentate gyrus (see text for details). Scale bar = 1 mm.

site along the transverse axis of the dentate gyrus, but is very prominent at levels rostral and caudal to the injection site. The associational projection from the rostral and middle portions of the dentate gyrus extends for as much as 80% of the full rostrocaudal extent of the dentate gyrus. The caudally directed projection is always more extensive and denser than the rostrally directed projection.

Cells in the polymorphic layer also give rise to so-called local projections to the outer two-thirds of the molecular layer. These local projections are most dense at the level of the cells of origin and extend for about 45% of the full rostrocaudal length of the dentate gyrus.

In the discussion that follows, we compare our findings on the topographical organization of the major connections of the monkey dentate gyrus with that previously described in rats. We conclude with a discussion of the functional implications of the topographical organization of these connections for the kind of information processing carried out by the dentate gyrus.

Mossy fibers

The topographical organization of the mossy fiber pathway in monkeys described in this study is largely consistent with that previously described for rodents (Blackstad et al., 1970; Gaarskjaer, 1978, 1981; Swanson et al., 1978; Amaral, 1979; Amaral and Dent, 1981; Claiborne et al., 1986; Amaral and Witter, 1989; Acsady et al., 1998; Seress et al., 2001; Buckmaster et al., 2002) and in humans (Lim et al., 1997). In monkeys, the mossy fibers first travel through the full transverse extent of the CA3 field of the hippocampus at approximately the same rostrocaudal level as the cells of origin but with a slight rostral inclination. Once they reach the distal portion of CA3, they change direction and extend for 3–5 mm toward the rostral pole of the hippocampus, or about 30% of the length of the monkey hippocampus. In rats, the mossy fibers also travel transversely through CA3 at approximately the same septotemporal level as the cells of origin, before extending for about 2 mm toward the temporal pole of the hippocampus, or about 20% of the length of the rat hippocampus. Note that the rostral portion of the monkey hippocampus corresponds to the temporal portion of the rat hippocampus.

In a unique study on the neuroanatomy of the human mossy fibers, Lim et al. (1997) found that the mossy fibers extend through the entire transverse extent of the CA3 pyramidal cell layer, as we have observed in the macaque monkey. Interestingly, they note that the mossy fibers are not oriented parallel to a single 800-μm. This is again consistent with our findings that in the monkey the mossy fibers have a slight rostral inclination through most of their transverse trajectory and then turn abruptly at the CA3/CA2 border to travel rostrally for several millimeters.

In contrast to the rat mossy fibers, the monkey mossy fibers do not travel in clearly defined suprapyramidal, intrapyramidal, and infrapyramidal bundles within CA3. Instead, the monkey mossy fibers appear to be completely interdigitated with the CA3 pyramidal cells. Fibers that are initially located deep to the pyramidal cell layer ascend through the pyramidal cell layer and travel to the distal portion of CA3 in a position superficial to the pyramidal cell layer. After the fibers complete their transverse trajectory, they turn and continue rostrally in the end bulb region. These species differences could simply reflect the fact that the monkey CA3 pyramidal cell layer is much wider and less well defined than that of the rat, especially in its proximal portion. The morphology of the monkey mossy fibers and terminals observed in this study was similar to that observed in rats (Claiborne et al., 1986), suggesting that the synaptic contacts between mossy fibers and CA3 pyramidal cells are largely similar between rodents and primates.

In rats, the mossy fibers terminate with specialized large presynaptic terminals on the proximal dendrites of mossy cells in the polymorphic layer and on the proximal dendrites of the pyramidal cells of the CA3 region of the hippocampus (Blackstad et al., 1970; Amaral, 1978, 1979; Gaarskjaer, 1978, 1981; Amaral and Dent, 1981; Ribak et al., 1985; Claiborne et al., 1986; Frotscher et al., 1991; Acsady et al., 1998). Mossy fibers also have thinner collaterals that give rise to typically sized presynaptic boutons, and these terminate preferentially on GABAergic

TABLE 2. Length of the Associational Projection Along the Rostrocaudal Axis

Case	AP ratio	Rostral (mm)	Caudal (mm)	Total length (mm)	Ratio to the dentate gyrus length
Rostral					
M0302-R	0.17	NA	NA	11.3 12.0 (Average)	0.72
M0202	0.20	1.7	11.3	13.0 11.8 (Median)	0.84
M1192-L	0.29	3.4	8.4	11.8 0.9 (SD)	0.86
Middle					
M1292	0.33	2.9	8.2	11.0 11.2 (Average)	0.81
M1192-R	0.33	3.6	7.7	11.3 11.0 (Median)	0.82
M0993	0.37	3.6	7.0	10.6 0.6 (SD)	0.74
M2792	0.44	4.6	6.0	10.6	0.80
M0903	0.45	3.6	5.3	12.0	0.64
M1093	0.46	5.0	7.0	12.0	0.82
M0401	0.56	6.0	5.0	11.0	0.81
Caudal					
M0903	0.77	3.8	2.2	6.0 6.3 (Average)	0.44
M1002	0.80	6.5	1.9	8.4 6.0 (Median)	0.58
M0703	0.89	4.1	0.5	4.6 1.9 (SD)	0.35

neurons in the polymorphic layer and CA3 region (Amaral, 1979; Frotscher, 1989; Acsady et al., 1998; Seress et al., 2001). We observed large mossy fiber expansions both in the polymorphic layer and in the CA3 region. In addition, smaller spherical varicosities were observed in the polymorphic layer and at the tips of thin filipodia that extend from the mossy fiber expansions. Our data are consistent with previous research (Frotscher et al., 1991; Seress, 2007) demonstrating that the distinctive thorny excrescences located on the proximal dendrites of mossy cells receive large mossy fiber terminals both in rodents and in primates, including humans. Thus, in all major characteristics, the mossy fibers that we observed in the macaque monkey resemble those that have been described for the rodent brain.

Associational projection

The topographical organization of the associational projection of the monkey dentate gyrus described here is also largely consistent with that previously described in rats (Blackstad, 1956; Zimmer, 1971; Fricke and Cowan, 1978; Swanson et al., 1978, 1981; Laurberg, 1979; Laurberg and Sorensen, 1981; Buckmaster et al., 1992, 1996). In rats, the associational projection originates primarily from mossy cells and innervates the inner one-third of the molecular layer. Autoradiographic studies in rats demonstrated that the peak density of the labeled axons and terminals of the associational projection is located in the inner one-third of the molecular layer (Fricke and Cowan, 1978; Kishi et al., 1980). As in the monkey, the associational connection terminates in a very modest way at the septotemporal level of origin and terminates with increasing density at progressively greater distances along the long axis (Amaral and Witter, 1989). In rats, injections in the middle septotemporal (rostrocaudal in the monkey) one-third of the dentate gyrus give rise to associational projections that are most extensively distributed along the septotemporal axis. Temporal injections, in contrast, produce projections that are restricted to the temporal portion of the dentate gyrus (Fricke and Cowan, 1978; Swanson et al., 1978). The monkey associational projection originates from mossy cells in the polymorphic layer (Buckmaster and Amaral, 2001) and terminates in the inner one-third of the molecular layer. This projection is virtually absent close to the cells of origin (<1–2 mm along the transverse or longitudinal axes of the dentate gyrus) but distributes widely, rostrally and caudally, to cover about 80% of the entire rostrocaudal length of the monkey dentate gyrus. In rats, the associational projection reaches about 75% of the length of the dentate gyrus (Amaral and Lavenex, 2007; Amaral et al., 2007).

In rodents, mossy cells have asymmetric synaptic contacts with mossy fibers (Amaral, 1978; Ribak et al., 1985; Frotscher et al., 1991; Blasco-Ibanez and Freund, 1997) and send axonal projections to the dendrites of the granule cells that also terminate with asymmetric synaptic contacts (Buckmaster et al., 1992, 1996; Blasco-Ibanez and Freund, 1997; Wenzel et al., 1997). These neuroanatomical findings have been validated through electrophysiological studies. The mossy cells receive inputs from granule cells and innervate interneurons in the polymorphic layer (Scharfman et al., 1990; Scharfman, 1995) and provide excitatory feedback projections to distant granule cells (Jackson and Scharfman, 1996). Thus, the associational projection constitutes an excitatory feedback circuit with granule cells that are distant from those contacting the mossy cells receiving the associational projection.

Local projections

The topographical organization of the so-called local projections of the monkey dentate gyrus described in this study is also largely consistent with that previously described in rodents (Bakst et al., 1986; Amaral and Witter, 1989; Leranth et al., 1990; Han et al., 1993; Buckmaster and Schwartzkroin, 1995; Sik et al., 1997; Buckmaster et al., 2002). Cells in the polymorphic layer give rise to projections to the outer two-thirds of the molecular layer. These projections were densest at the level of the cells of origin, and heavy labeling decreased greatly within approximately 1.5–2 mm rostrally and caudally to the cells of origin. Nevertheless, more meager local projections extended for about 45% of the full rostrocaudal length of the dentate gyrus. At least some of these fibers have been shown to be immunoreactive for GABA and somatostatin in rats (Bakst et al., 1986), monkeys (Bakst et al., 1985), and humans (Amaral et al., 1988). In rats, the GABA/somatostatin projection also terminates most heavily around the level of the cells of origin, and termination rapidly decreases within approximately 1.5 mm septally and temporally to the cells of origin. In rats, the somatostatin-immunoreactive cells in the polymorphic layer that give rise to the local projections are contacted by mossy fiber termi-

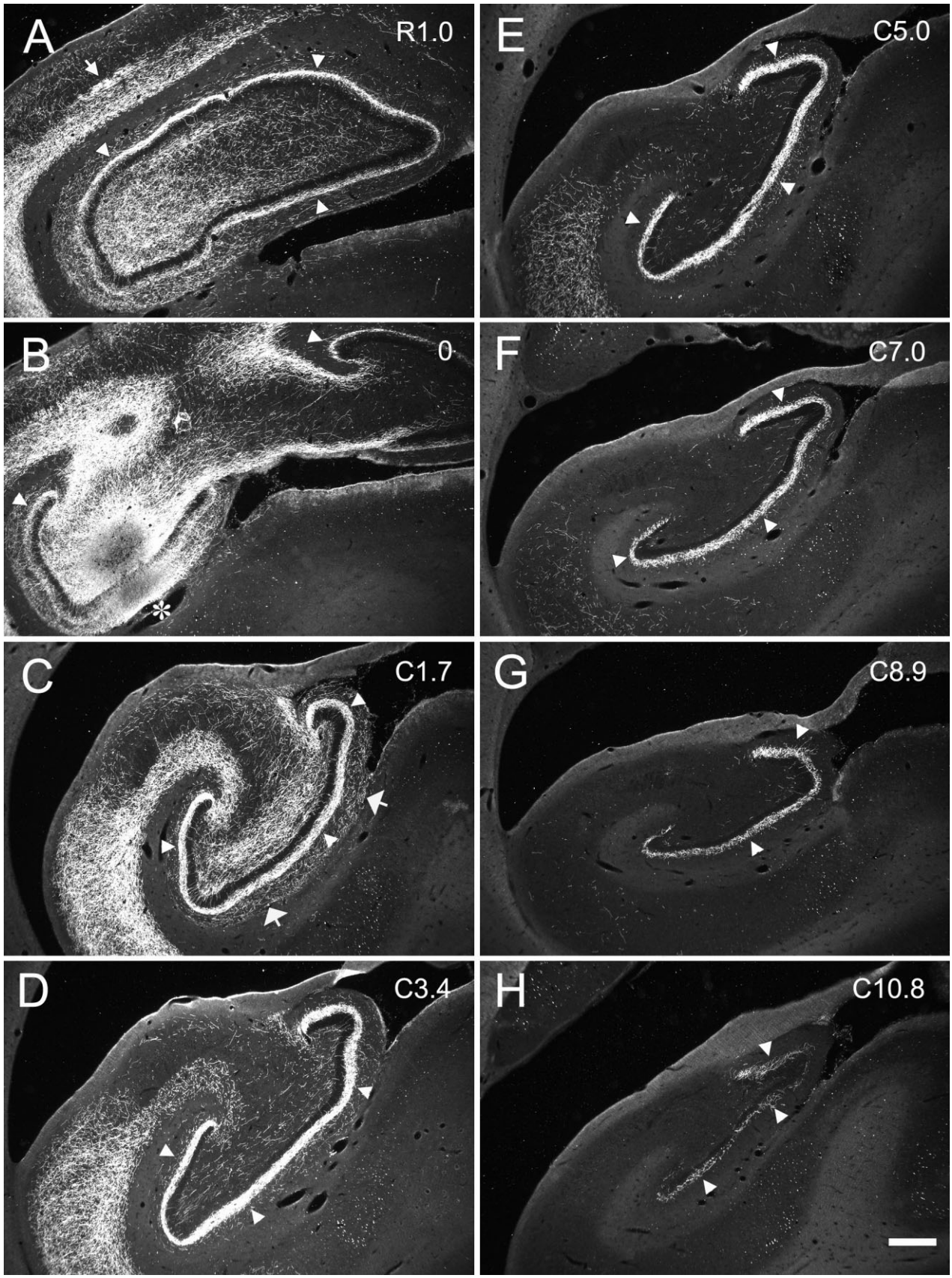

Fig. 11. **A–H:** Darkfield photomicrographs of coronal sections of the dentate gyrus arranged from rostral (A) to caudal (H) showing the distribution of PHA-L-labeled fibers and terminals in case M-02-02. The injection was located in the rostral one-third of the dentate gyrus (asterisk in B). Note that the associational projection travels throughout almost the full rostrocaudal extent of the hippocampus (arrowheads). Scale bar = 0.5 mm.

TABLE 3. Length of the Local Projection Along the Rostrocaudal Axis

Case	AP ratio	Rostral (mm)	Caudal (mm)	Total length (mm)	Ratio to the dentate gyrus length
Rostral					
M0202	0.20	1.7	7.2	8.9 7.7 (Average)	0.58
M1192-L	0.29	2.6	3.8	6.5 7.7 (Median)	0.47
Middle				1.7 (SD)	
M1292	0.33	2.9	4.6	7.4	0.54
M1192-R	0.33	3.1	1.9	5.0 5.6 (Average)	0.37
M0993	0.37	2.4	5.0	7.4 5.0 (Median)	0.52
M2792	0.44	1.4	2.4	3.8 1.9 (SD)	0.29
M0903	0.45	1.4	1.7	3.1	0.22
M1093	0.46	4.1	3.8	7.9	0.54
M0401	0.56	2.6	1.9	4.6	0.33
Caudal					
M0903	0.77	3.6	2.2	5.8 6.7 (Average)	0.42
M1002	0.80	6.2	1.9	8.2 6.4 (Median)	0.56
M0703	0.89	6.2	0.5	6.7 1.1 (SD)	0.52
M0402	0.91	4.8	1.2	6.0	0.46

nals (Leranth et al., 1990) and form inhibitory synaptic contacts with the granule cell dendrites at the level near their origin (Bakst et al., 1986; Amaral and Witter, 1989; Leranth et al., 1990; Buckmaster and Schwartzkroin, 1995; Katona et al., 1999; Buckmaster et al., 2002). Thus, the local projections constitute an inhibitory feedback circuit to the granule cells within a relatively restricted region of the dentate gyrus.

Functional considerations

The topographical organization of the major connections of the monkey dentate gyrus has very strong implications for the functional processes carried out by this brain region. In particular, the topographical organization of these circuits along the long axis of the hippocampus dictates how different types of information reaching various rostrocaudal levels of the dentate gyrus can be integrated. We have previously emphasized that the network of intrinsic connections of the hippocampal formation is organized in three dimensions. The longitudinal component of the network is every bit as substantial as the transverse or "lamellar" component (Amaral and Witter, 1989). Although the neuroanatomical validity of this concept has been demonstrated on numerous occasions, the physiological interpretation of the neuroanatomy remains to be clarified (Andersen et al., 2000). Nonetheless, there is substantial electrophysiological data available indicating that the intrinsic circuitry of the hippocampal formation supports longitudinal distribution of information both within the dentate gyrus (Hetherington et al., 1994; Sloviter and Brisman, 1995; Zappone and Sloviter, 2004) and from the entorhinal cortex to other fields of the hippocampal formation (Bartesaghi et al., 1983; Pare and Llinas, 1994). Indeed, we have previously shown both in the rat (Dolorfo and Amaral, 1998) and in the macaque monkey (Witter et al., 1989; Witter and Amaral, 1991) that different portions of the entorhinal cortex project to different regions of the dentate gyrus. In the monkey, the medial portion of the entorhinal cortex projects to the rostral dentate gyrus; the midmediolateral portion of the entorhinal cortex projects to midrostrocaudal dentate gyrus; and the lateral portion of the entorhinal cortex projects to the caudal dentate gyrus. Consequently, the mossy fibers, the associational projection, and the local projections will contribute in very different ways to the further distribution of these inputs along the rostrocaudal axis of the dentate gyrus.

We have confirmed in the monkey that the granule cells of the dentate gyrus originate the mossy fibers, which project first to a very restricted portion of the polymorphic layer and then along the transverse axis of the CA3 field of the hippocampus. In the polymorphic layer, the mossy fibers establish asymmetric (excitatory) contacts with mossy cells located very close to the cells of origin (Ribak et al., 1985; Frotscher et al., 1991; Blasco-Ibanez and Freund, 1997). This projection is also restricted along the transverse axis of the dentate gyrus, and mossy fibers originating in the infrapyramidal blade of the dentate gyrus have a lower probability of contacting mossy cells subjacent to the suprapyramidal blade, or vice versa. The mossy fiber projection toward the CA3 pyramidal cells first follows a transverse trajectory with a slight rostral inclination that does not exceed 1 mm, or about 5% of the entire rostrocaudal length of the hippocampus. After reaching the distal end of CA3, the mossy fibers turn rostrally and travel for about 30% of the entire length of the hippocampus. Consequently, the pyramidal cells located in the proximal and middle portions of CA3 receive mossy fiber input from only a very restricted region of the dentate gyrus located at the same rostrocaudal level. In contrast, the pyramidal cells located in the distal portion of CA3 receive mossy fiber inputs from granule cells both from their own rostrocaudal level and from granule cells located as far caudally as one-third of the entire length of the dentate gyrus. This portion of the mossy fiber projection appears to be almost entirely ignored in functional analyses of the hippocampal formation, although it has been known for many decades (Lorente de Nó, 1934; Kilmer and McLardy, 1970). Consequently, there is a very strong directionality, from caudal to rostral, in the transfer of whatever information is carried by the mossy fibers. Moreover, this information is transmitted only to the pyramidal neurons located in the distal portion of CA3 and not to the pyramidal neurons located in the proximal and mid portion of CA3. The topography of the mossy fiber projections along the long axis of the hippocampus therefore suggests the existence of functionally distinct domains along the transverse axis of CA3.

The mossy cells located in the polymorphic layer originate the associational projection to the inner one-third of

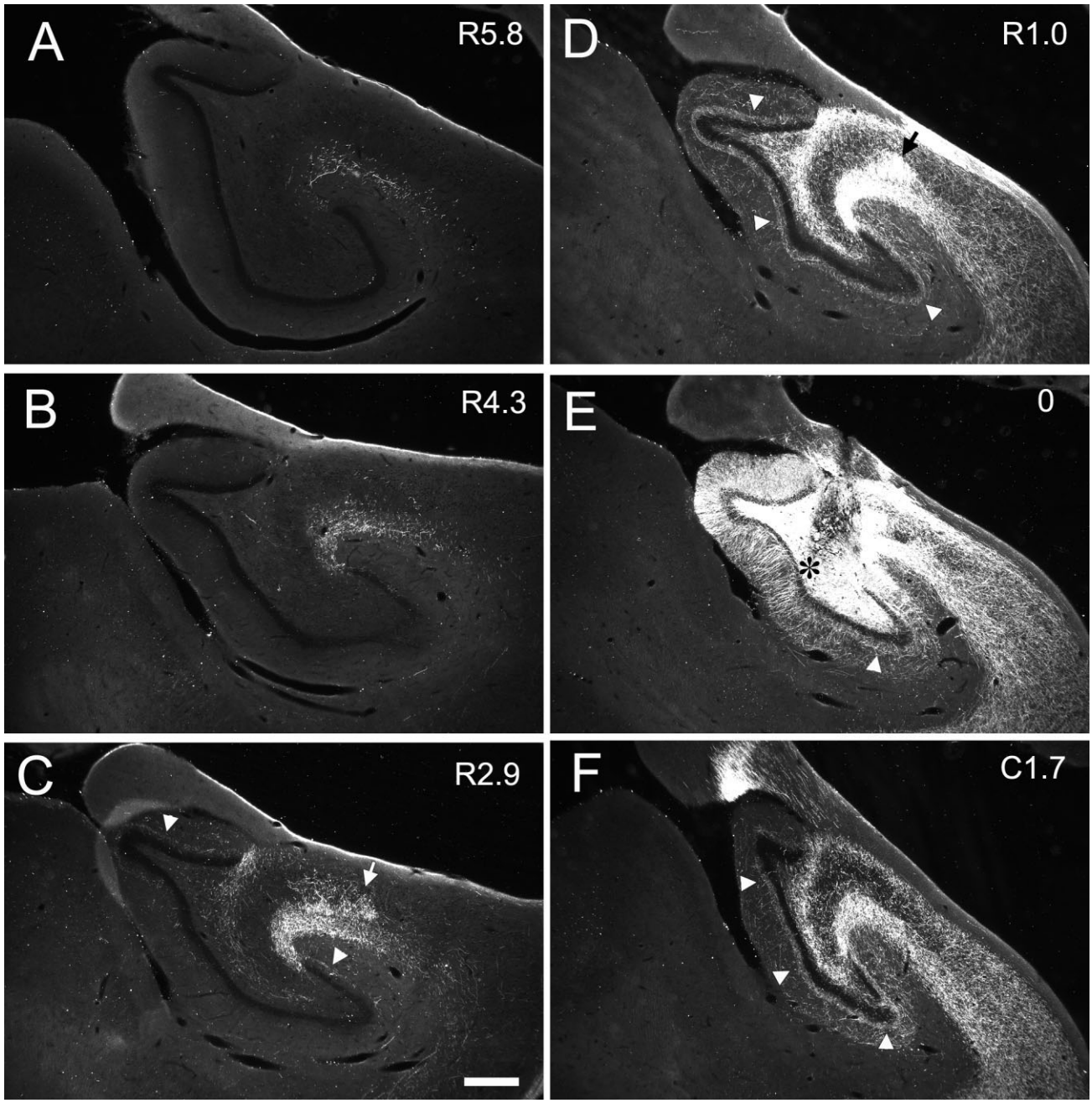

Fig. 12. **A–F:** Darkfield photomicrographs of coronal sections of the dentate gyrus, arranged from rostral (A) to caudal (F), showing the distribution of BDA-labeled fibers and terminals in case M-09-03-R. The injection was located in the caudal portion of the dentate gyrus (asterisk in E). Note that the mossy fibers are visible rostral to the injection site (arrows), whereas the associational projections travel both rostrally and caudally (arrowheads). Scale bar = 0.5 mm.

the molecular layer. Mossy cells establish asymmetric (excitatory) synaptic contacts with the proximal portion of the dendrites of the dentate granule cells located at a distance from the cells of origin to cover more than 80% of the entire rostrocaudal length of the dentate gyrus. Interestingly, the projection directed caudally is stronger than the projection directed rostrally. Although this asymmetry is clearly not as pronounced as for the mossy fiber projections, it suggests some directionality in the transfer of information from rostral to caudal through the associational projection. Inputs reaching any particular level of the dentate gyrus will exert a feed-forward excitatory influence over much of the long axis of the dentate gyrus. However, inputs reaching the rostral portion of the dentate gyrus will have a greater excitatory influence over the caudal portion of the dentate

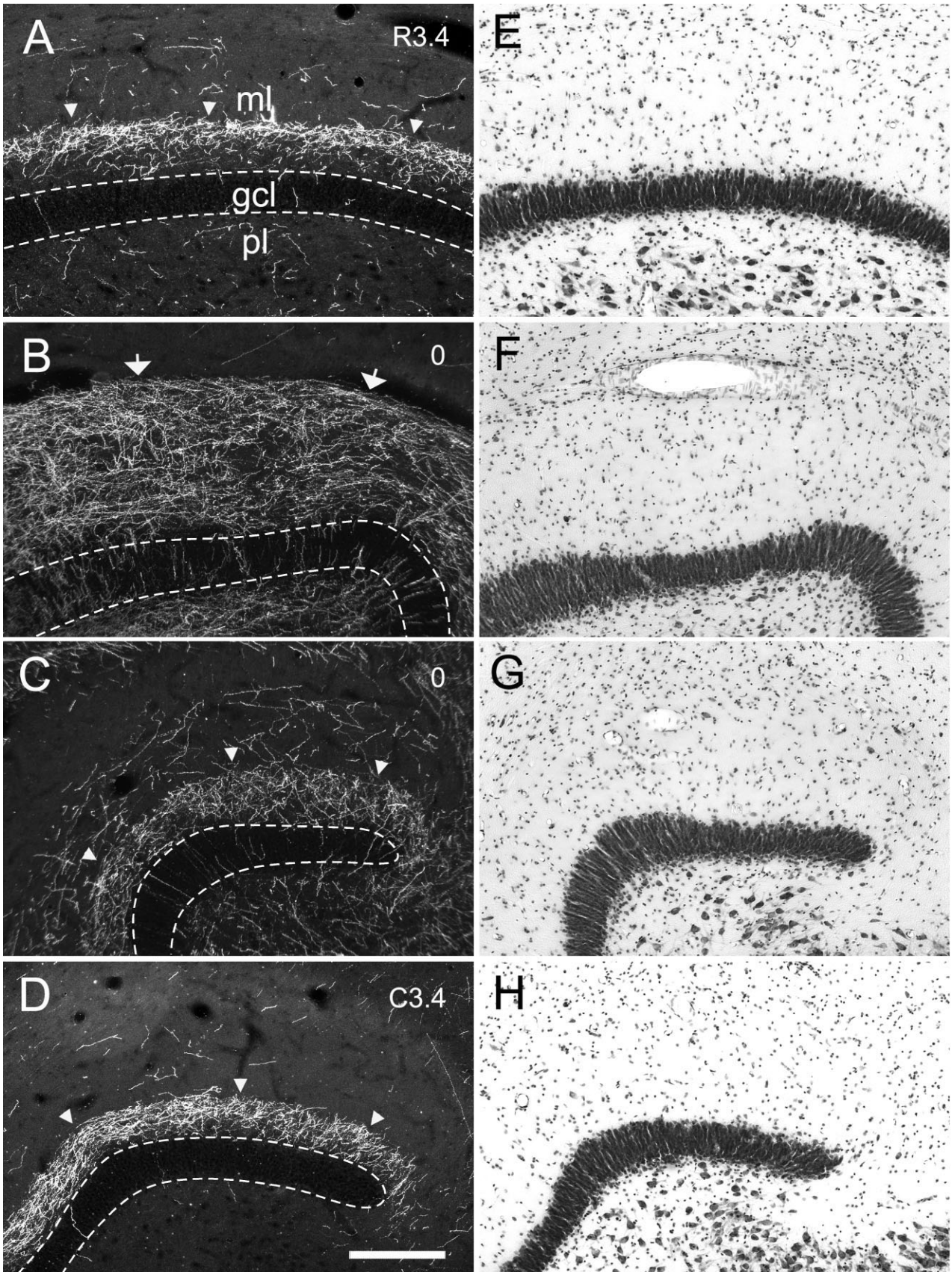

Fig. 13. High-magnification photomicrographs of coronal sections showing the laminar distribution of PHA-L-labeled associational and local projections in the molecular layer of the dentate gyrus (case M-10-93). Labeled fibers and terminals were located near the injection site (B) and at some distance away from it (C) at the level of the injection site. The labeling is also shown in the section rostral (A) and caudal (D) to the injection site. Nissl-stained sections (**E–H**) are adjacent to the PHA-L-labeled sections (**A–D**). The dashed lines indicate the borders of the granule cell layer. The regions taken for photomicrographs are indicated by white rectangles in Figure 7 (A corresponds to the rectangle in Fig. 7B; B and C correspond to the rectangles in Fig. 7E; D corresponds to the rectangle in Fig. 7G). Note that the associational projection heavily innervates the inner one-third of the molecular layer away from the injection site (A,D). In contrast, the local projections terminate more densely in the outer two-thirds of the molecular layer and closer to the injection site (B). Scale bar = 0.25 mm.

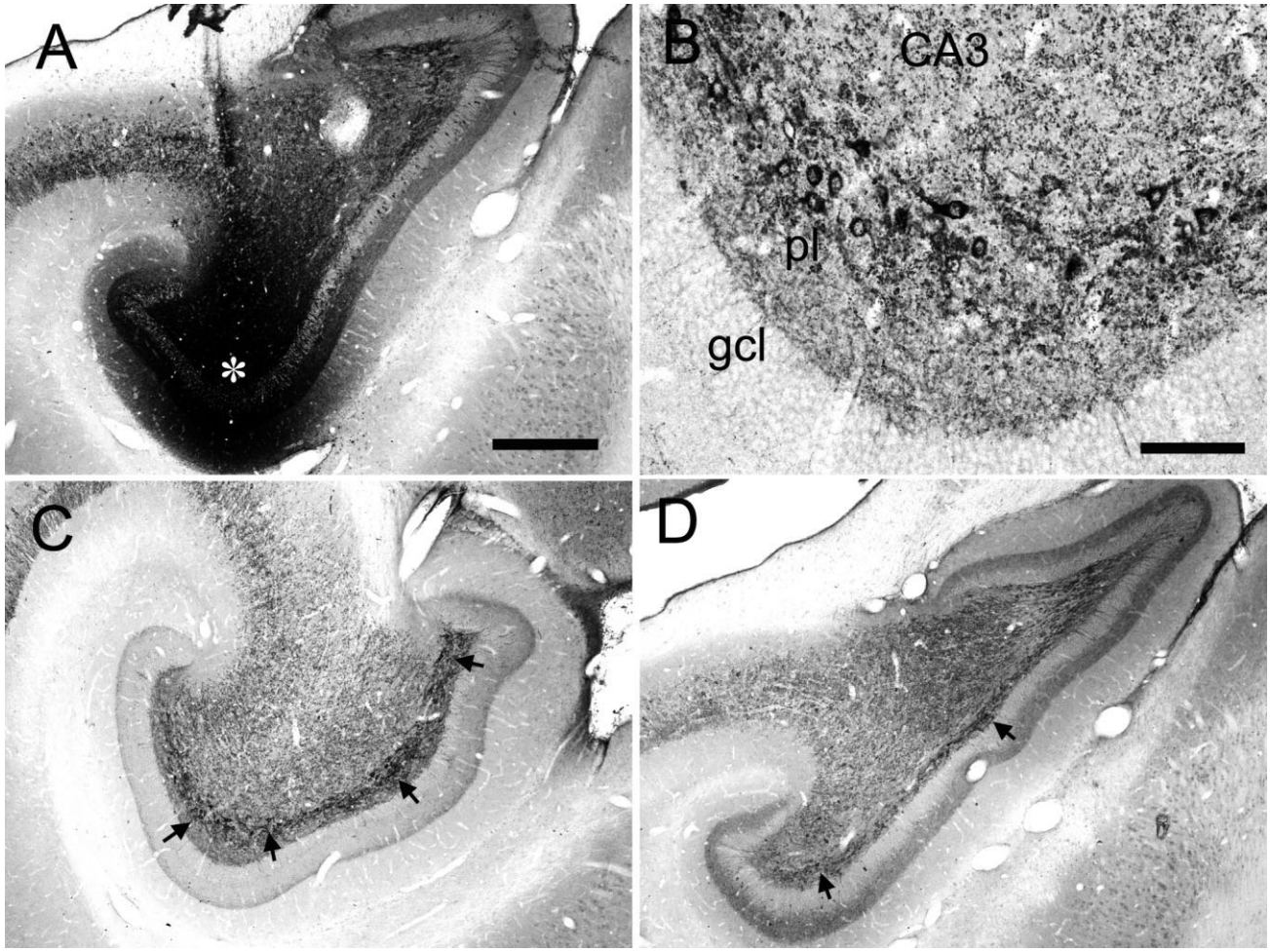

Fig. 14. Brightfield photomicrographs showing the retrogradely labeled cells in the polymorphic layer of the dentate gyrus following a CTB injection in the dentate gyrus (case M-04-02-L). **A:** The CTB injection is indicated by an asterisk. **B:** High-magnification photomicrograph showing CTB-labeled cells in the polymorphic layer. Representative sections located 3.8 mm rostral (**C**) and 1.4 mm caudal (**D**) to the injection site. Large numbers of retrogradely labeled cells are located rostral to the injection site (C). The arrows indicate the region of dense retrogradely labeled cells in the polymorphic layer of the dentate gyrus. Scale bars = 0.5 mm in A (applies to A,C,D); 100 μm in B.

gyrus than inputs reaching the caudal portion of the dentate gyrus will have over the rostral portion of the dentate gyrus. Although we infer that the synaptic effect would be excitatory, it may well be that the monosynaptic excitatory input is onto both excitatory and inhibitory neurons. Thus, the net effect may actually be inhibitory on granule cell activity at distant levels (Zappone and Sloviter, 2004). In fact, the axons of the mossy cells were shown to contact GABAergic interneurons in the polymorphic layer as well as dendrites of the granule cells (Scharfman et al., 1990; Wenzel et al., 1997). The existence of such an extensive network of associational connections raises some interesting questions regarding the origin of functional domains that are believed to exist along the longitudinal axis of the hippocampus (Colombo et al., 1998; Moser and Moser, 1998; Small, 2002; Bannerman et al., 2004; Daselaar et al., 2006; Strange and Dolan, 2006; Chua et al., 2007). Indeed, the organization of the intrinsic connectivity of the dentate gyrus suggests an increased integration of information rather than a segregation of function within the hippocampal circuit (Lavenex and Amaral, 2000). Previous anatomical studies in rats indicate that cells of the polymorphic layer also give rise to a prominent commissural projection that terminates in the inner portion of the contralateral molecular layer (Blackstad, 1956; Hjorth-Simonsen and Laurberg, 1977; Laurberg, 1979; Laurberg and Sorensen, 1981; Swanson et al., 1981; Deller et al., 1996). In the monkey, the commissural connection is present only in the rostral portion of the dentate gyrus (Amaral et al., 1984; Demeter et al., 1985). This finding suggests that a very limited interaction between the left and the right hippocampi could further support hemispheric specialization in the primate brain (Milner, 1970). Although we have not observed any difference in the neuroanatomical organization of the left and right hippocampi, cortical inputs from specialized areas in the

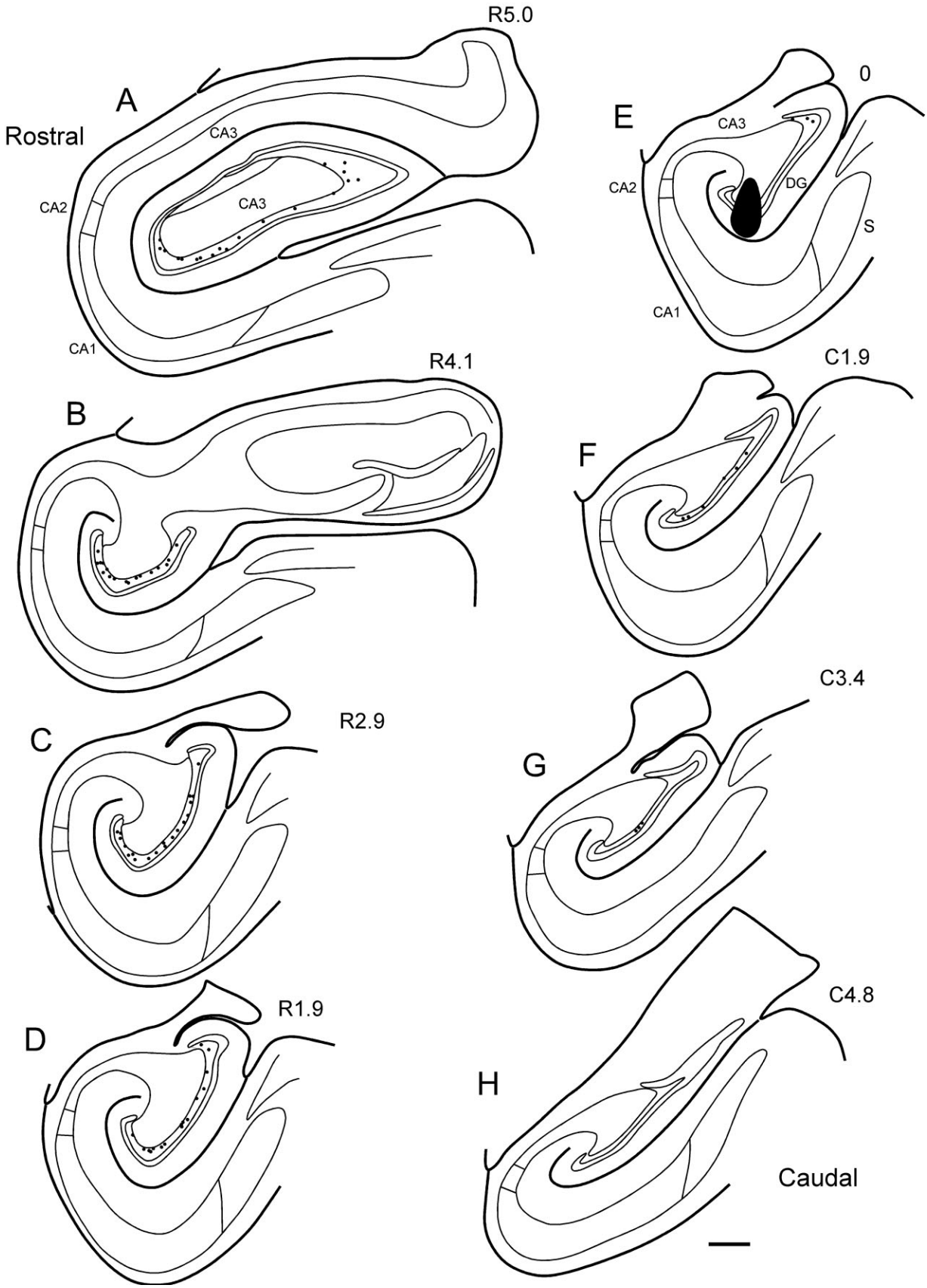

Fig. 15. **A–H:** Series of line drawings of coronal sections illustrating the distribution of retrogradely labeled cells (black dots) in the polymorphic layer after a CTB injection in the dentate gyrus (case M-04-02-L). The injection site was located at a midrostrocaudal level of the dentate gyrus. Note that the labeled cells in CA3 and the granule cell layer of the dentate gyrus were omitted. The sections are arranged from rostral (A) to caudal (H). Note that the labeled cells are distributed very widely in the rostrocaudal direction, although larger numbers of retrogradely labeled cells are located rostral to the level of the injection site. Scale bar = 1 mm.

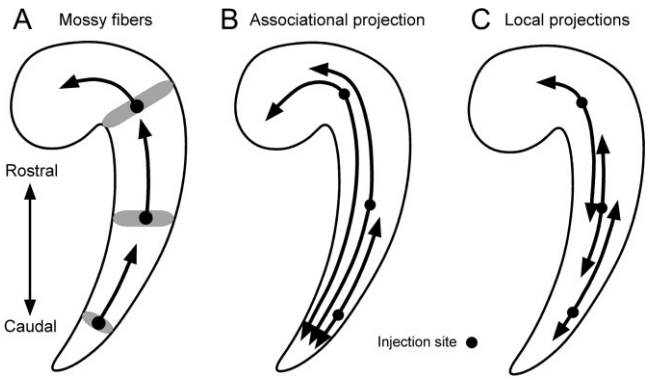

Fig. 16. Summary diagram of the mossy fibers (**A**), associational projection (**B**), and local projections (**C**) along the rostrocaudal axis of the dentate gyrus and hippocampus. The injection site is represented by a circle. The rostrocaudal extent of each projection is shown by an arrow. Each projection is illustrated originating from the rostral, middle, and caudal levels of the dentate gyrus. A: The shaded area indicates the transverse component of the mossy fiber projections. Note that, irrespective of the rostrocaudal level of the injection, the mossy fibers always travel for 3–5 mm in the rostral direction within distal CA3, or about 33% of the full length of the hippocampus. The associational projection always extends widely both rostrally and caudally. Projections originating from the mid- and rostral portions of the dentate gyrus extend for about 80% of the rostrocaudal extent of the dentate gyrus. Associational projections originating in the caudal one-third of the dentate gyrus are more restricted in their rostrocaudal extent and cover about 45% of the length of the dentate gyrus. The local projections also extend for about 45% of the full length of the dentate gyrus and are therefore less extensive than the associational projection.

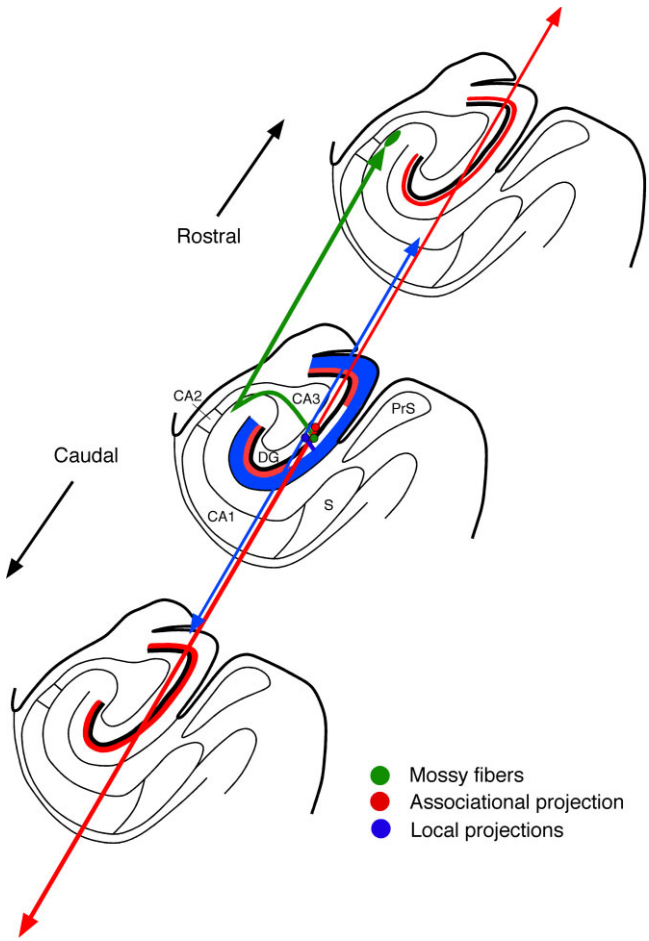

Fig. 17. Summary diagram showing the topographical organization of the major connections of the dentate gyrus, including the mossy fibers (green), associational projections (red), and local projections (blue). Note that each projection has an extensive distribution along the longitudinal axis. The mossy fibers travel transversely, but slightly rostrally, in the proximal and middle portions of CA3 and, at the distal portion of CA3, change direction and travel rostrally for 3–5 mm. The associational projection travels widely both rostrally and caudally, terminating in the inner one-third of the molecular layer. The projection is absent or weak near the injection and is dense outside the injection. In contrast, the local projections to the outer two-thirds of the molecular layer are denser near the injection site.

two hemispheres could be treated independently by the right and left hippocampi in primates.

Other cells in the polymorphic layer of the dentate gyrus originate the so-called local projections to the outer two-thirds of the molecular layer. These cells establish symmetric (inhibitory) synaptic contacts with the distal portion of the dendrites of the granule cells located relatively close to the cells of origin. These projections are heaviest in a zone covering about 20% of the length of the dentate gyrus, although additional lighter projections cover as much as 45% of the entire length of the dentate gyrus. This inhibitory feedback circuit has the potential to reduce the excitability of granule cells within a relatively restricted region of the dentate gyrus and therefore permits the induction of a sparser coding of information within the dentate gyrus (Acsady and Kali, 2007). Specific sparse coding of information is believed to be fundamental for the purported role of the dentate gyrus in the process of pattern separation (Chawla et al., 2005; Rolls and Kesner, 2006).

ACKNOWLEDGMENTS

This research was conducted, in part, at the California National Primate Research Center (NIH grant RR00169). The authors thank Jeffrey L. Bennett and Pamela C. Tennant for surgical and immunohistochemical assistance and José R. Alonso, Jennifer L. Freese, Pamela Banta Lavenex, Brian W. Leonard, Lisa Stefanacci, and Wendy A. Suzuki for surgical assistance.

LITERATURE CITED

Acsady L, Kali S. 2007. Models, structure, function: the transformation of cortical signals in the dentate gyrus. Prog Brain Res 163:577–599.

Acsady L, Kamondi A, Sik A, Freund T, Buzsaki G. 1998. GABAergic cells are the major postsynaptic targets of mossy fibers in the rat hippocampus. J Neurosci 18:3386–3403.

Amaral DG. 1978. A Golgi study of cell types in the hilar region of the hippocampus in the rat. J Comp Neurol 182:851–914.

Amaral DG. 1979. Synaptic extensions from the mossy fibers of the fascia dentata. Anat Embryol 155:241–251.

Amaral DG, Dent JA. 1981. Development of the mossy fibers of the dentate gyrus: I. A light and electron microscopic study of the mossy fibers and their expansions. J Comp Neurol 195:51–86.

Amaral DG, Lavenex P. 2007. Hippocampal neuroanatomy. In: Andersen P, Morris R, Amaral D, Bliss T, O'Keefe J, editors. The hippocampus book. New York: Oxford University Press. p 37–114.

Amaral DG, Witter MP. 1989. The three-dimensional organization of the

hippocampal formation: a review of anatomical data. Neuroscience 31:571–591.

Amaral DG, Insausti R, Cowan WM. 1984. The commissural connections of the monkey hippocampal formation. J Comp Neurol 224:307–336.

Amaral DG, Insausti R, Campbell MJ. 1988. Distribution of somatostatin immunoreactivity in the human dentate gyrus. J Neurosci 8:3306–3316.

Amaral DG, Scharfman HE, Lavenex P. 2007. The dentate gyrus: fundamental neuroanatomical organization (dentate gyrus for dummies). Prog Brain Res 163:3–790.

Andersen P, Soleng AF, Raastad M. 2000. The hippocampal lamella hypothesis revisited. Brain Res 886:165–171.

Bakst I, Morrison JH, Amaral DG. 1985. The distribution of somatostatin-like immunoreactivity in the monkey hippocampal formation. J Comp Neurol 236:423–442.

Bakst I, Avendano C, Morrison JH, Amaral DG. 1986. An experimental analysis of the origins of somatostatin-like immunoreactivity in the dentate gyrus of the rat. J Neurosci 6:1452–1462.

Bannerman DM, Rawlins JN, McHugh SB, Deacon RM, Yee BK, Bast T, Zhang WN, Pothuizen HH, Feldon J. 2004. Regional dissociations within the hippocampus—memory and anxiety. Neurosci Biobehav Rev 28:273–283.

Banta-Lavenex P, Amaral DG, Lavenex P. 2006. Hippocampal lesion prevents spatial relational learning in adult macaque monkeys. J Neurosci 26:4546–4558.

Bartesaghi R, Gessi T, Sperti L. 1983. Interlamellar transfer of impulses in the hippocampal formation. Exp Neurol 82:550–567.

Blackstad TW. 1956. Commissural connections of the hippocampal region in the rat, with special reference to their mode of termination. J Comp Neurol 105:417–537.

Blackstad TW, Brink K, Hem J, Jeune B. 1970. Distribution of hippocampal mossy fibers in the rat. An experimental study with silver impregnation methods. J Comp Neurol 138:433–449.

Blasco-Ibanez JM, Freund TF. 1997. Distribution, ultrastructure, and connectivity of calretinin-immunoreactive mossy cells of the mouse dentate gyrus. Hippocampus 7:307–320.

Buckmaster PS, Amaral DG. 2001. Intracellular recording and labeling of mossy cells and proximal CA3 pyramidal cells in macaque monkeys. J Comp Neurol 430:264–281.

Buckmaster PS, Schwartzkroin PA. 1995. Interneurons and inhibition in the dentate gyrus of the rat in vivo. J Neurosci 15:774–789.

Buckmaster PS, Strowbridge BW, Kunkel DD, Schmiege DL, Schwartzkroin PA. 1992. Mossy cell axonal projections to the dentate gyrus molecular layer in the rat hippocampal slice. Hippocampus 2:349–362.

Buckmaster PS, Wenzel HJ, Kunkel DD, Schwartzkroin PA. 1996. Axon arbors and synaptic connections of hippocampal mossy cells in the rat in vivo. J Comp Neurol 366:271–292.

Buckmaster PS, Yamawaki R, Zhang GF. 2002. Axon arbors and synaptic connections of a vulnerable population of interneurons in the dentate gyrus in vivo. J Comp Neurol 445:360–373.

Chawla MK, Guzowski JF, Ramirez-Amaya V, Lipa P, Hoffman KL, Marriott LK, Worley PF, McNaughton BL, Barnes CA. 2005. Sparse, environmentally selective expression of Arc RNA in the upper blade of the rodent fascia dentata by brief spatial experience. Hippocampus 15:579–586.

Chua EF, Schacter DL, Rand-Giovannetti E, Sperling RA. 2007. Evidence for a specific role of the anterior hippocampal region in successful associative encoding. Hippocampus 17:1071–1080.

Claiborne BJ, Amaral DG, Cowan WM. 1986. A light and electron microscopic analysis of the mossy fibers of the rat dentate gyrus. J Comp Neurol 246:435–458.

Colombo M, Fernandez T, Nakamura K, Gross CG. 1998. Functional differentiation along the anterior-posterior axis of the hippocampus in monkeys. J Neurophysiol 80:1002–1005.

Daselaar SM, Fleck MS, Cabeza R. 2006. Triple dissociation in the medial temporal lobes: recollection, familiarity, and novelty. J Neurophysiol 96:1902–1911.

Deller T, Nitsch R, Frotscher M. 1996. Heterogeneity of the commissural projection to the rat dentate gyrus: a *Phaseolus vulgaris* leucoagglutinin tracing study. Neuroscience 75:111–121.

Demeter S, Rosene DL, Van Hoesen GW. 1985. Interhemispheric pathways of the hippocampal formation, presubiculum, and entorhinal and posterior parahippocampal cortices in the rhesus monkey: the structure and organization of the hippocampal commissures. J Comp Neurol 233:30–47.

Dolorfo CL, Amaral DG. 1998. Entorhinal cortex of the rat: topographic organization of the cells of origin of the perforant path projection to the dentate gyrus. J Comp Neurol 398:25–48.

Fricke R, Cowan WM. 1978. An autoradiographic study of the commissural and ipsilateral hippocampo-dentate projections in the adult rat. J Comp Neurol 181:253–269.

Frotscher M, Seress L, Schwerdtfeger WK, Buhl E. 1991. The mossy cells of the fascia dentata: a comparative study of their fine structure and synaptic connections in rodents and primates. J Comp Neurol 312:145–163.

Gaarskjaer FB. 1978. Organization of the mossy fiber system of the rat studied in extended hippocampi. II. Experimental analysis of fiber distribution with silver impregnation methods. J Comp Neurol 178:73–88.

Gaarskjaer FB. 1981. The hippocampal mossy fiber system of the rat studied with retrograde tracing techniques. Correlation between topographic organization and neurogenetic gradients. J Comp Neurol 203:717–735.

Gall C. 1984. The distribution of cholecystokinin-like immunoreactivity in the hippocampal formation of the guinea pig: localization in the mossy fibers. Brain Res 306:73–83.

Han ZS, Buhl EH, Lorinczi Z, Somogyi P. 1993. A high degree of spatial selectivity in the axonal and dendritic domains of physiologically identified local-circuit neurons in the dentate gyrus of the rat hippocampus. Eur J Neurosci 5:395–410.

Hetherington PA, Austin KB, Shapiro ML. 1994. Ipsilateral associational pathway in the dentate gyrus: an excitatory feedback system that supports N-methyl-D-aspartate-dependent long-term potentiation. Hippocampus 4(4):422–438.

Hjorth-Simonsen A, Laurberg S. 1977. Commissural connections of the dentate area in the rat. J Comp Neurol 174:591–606.

Jackson MB, Scharfman HE. 1996. Positive feedback from hilar mossy cells to granule cells in the dentate gyrus revealed by voltage-sensitive dye and microelectrode recording. J Neurophysiol 76:601–616.

Katona I, Acsady L, Freund TF. 1999. Postsynaptic targets of somatostatin-immunoreactive interneurons in the rat hippocampus. Neuroscience 88:37–55.

Kilmer WL, McLardy T. 1970. A model of hippocampal CA3 circuitry. Int J Neurosci 1:107–112.

Kishi K, Stanfield BB, Cowan WM. 1980. A quantitative EM autoradiographic study of the commissural and associational connections of the dentate gyrus in the rat. Anat Embryol 160:173–186.

Laurberg S. 1979. Commissural and intrinsic connections of the rat hippocampus. J Comp Neurol 184:685–708.

Laurberg S, Sorensen KE. 1981. Associational and commissural collaterals of neurons in the hippocampal formation (hilus fasciae dentatae and subfield CA3). Brain Res 212:287–300.

Lavenex P, Amaral DG. 2000. Hippocampal–neocortical interaction: a hierarchy of associativity. Hippocampus 10:420–430.

Lavenex P, Suzuki WA, Amaral DG. 2004. Perirhinal and parahippocampal cortices of the macaque monkey: Intrinsic projections and interconnections. J Comp Neurol 472:371–394.

Leranth C, Malcolm AJ, Frotscher M. 1990. Afferent and efferent synaptic connections of somatostatin-immunoreactive neurons in the rat fascia dentata. J Comp Neurol 295:111–122.

Lim C, Blume HW, Madsen JR, Saper CB. 1997. Connections of the hippocampal formation in humans: I. The mossy fiber pathway. J Comp Neurol 385:325–351.

Lorente de Nó R. 1934. Studies on the structure of the cerebral cortex. II. Continuation of the study of the ammonic system. J Psychol Neurol 46:113–177.

Milner B. 1970. Memory and the medial temporal regions of the brain. In: Pribram KH, Broadbent DE, editors. Biology of memory. New York: Academic Press. p 29–50.

Milner B, Squire LR, Kandel ER. 1998. Cognitive neuroscience and the study of memory. Neuron 20:445–468.

Moser MB, Moser EI. 1998. Functional differentiation in the hippocampus. Hippocampus 8:608–619.

Pare D, Llinas R. 1994. Non-lamellar propagation of entorhinal influences in the hippocampal formation: multiple electrode recordings in the isolated guinea pig brain in vitro. Hippocampus 4:403–409.

Pitkanen A, Amaral DG. 1993. Distribution of parvalbumin-immunoreactive cells and fibers in the monkey temporal lobe: the hippocampal formation. J Comp Neurol 331:37–74.

Ribak CE, Seress L, Amaral DG. 1985. The development, ultrastructure and synaptic connections of the mossy cells of the dentate gyrus. J Neurocytol 14:835–857.

Rolls ET, Kesner RP. 2006. A computational theory of hippocampal function, and empirical tests of the theory. Prog Neurobiol 79:1–48.

Rosene DL, Van Hoesen GW. 1977. Hippocampal efferents reach widespread areas of cerebral cortex and amygdala in the rhesus monkey. Science 198:315–317.

Rosene DL, Van Hoesen GW. 1987. The hippocampal formation of the primate brain. A review of some comparative aspects of cytoarchitecture and connections. In: Jones EG, Peters A, editors. Cerebral cortex. New York: Plenum Publishing. p 345–456.

Sandler R, Smith AD. 1991. Coexistence of GABA and glutamate in mossy fiber terminals of the primate hippocampus: an ultrastructural study. J Comp Neurol 303:177–192.

Scharfman HE. 1995. Electrophysiological evidence that dentate hilar mossy cells are excitatory and innervate both granule cells and interneurons. J Neurophysiol 74:179–194.

Scharfman HE, Kunkel DD, Schwartzkroin PA. 1990. Synaptic connections of dentate granule cells and hilar neurons: results of paired intracellular recordings and intracellular horseradish peroxidase injections. Neuroscience 37:693–707.

Seress L. 2007. Comparative anatomy of the hippocampal dentate gyrus in adult and developing rodents, nonhuman primates and humans. Prog Brain Res 163:23–41.

Seress L, Abraham H, Paleszter M, Gallyas F. 2001. Granule cells are the main source of excitatory input to a subpopulation of GABAergic hippocampal neurons as revealed by electron microscopic double staining for zinc histochemistry and parvalbumin immunocytochemistry. Exp Brain Res 136:456–462.

Seress L, Abraham H, Czeh B, Fuchs E, Leranth C. 2008. Calretinin expression in hilar mossy cells of the hippocampal dentate gyrus of nonhuman primates and humans. Hippocampus 18:425–434.

Sik A, Penttonen M, Buzsaki G. 1997. Interneurons in the hippocampal dentate gyrus: an in vivo intracellular study. Eur J Neurosci 9:573–588.

Sloviter RS, Brisman JL. 1995. Lateral inhibition and granule cell synchrony in the rat hippocampal dentate gyrus. J Neurosci 15:811–820.

Small SA. 2002. The longitudinal axis of the hippocampal formation: its anatomy, circuitry, and role in cognitive function. Rev Neurosci 13: 183–194.

Squire LR, Zola SM. 1996. Structure and function of declarative and nondeclarative memory systems. Proc Natl Acad Sci U S A 93:13515–13522.

Storm-Mathisen J, Fonnum F. 1972. Localization of transmitter candidates in the hippocampal region. Prog Brain Res 36:41–58.

Strange BA, Dolan RJ. 2006. Anterior medial temporal lobe in human cognition: memory for fear and the unexpected. Cognit Neuropsychiatry 11:198–218.

Swanson LW, Wyss JM, Cowan WM. 1978. An autoradiographic study of the organization of intrahippocampal association pathways in the rat. J Comp Neurol 181:681–715.

Swanson LW, Sawchenko PE, Cowan WM. 1981. Evidence for collateral projections by neurons in Ammon's horn, the dentate gyrus, and the subiculum: a multiple retrograde labeling study in the rat. J Neurosci 1:548–559.

Szabo J, Cowan WM. 1984. A stereotaxic atlas of the brain of the cynomolgus monkey (*Macaca fascicularis*). J Comp Neurol 222:265–300.

van Daal JH, Zanderink HE, Jenks BG, van Abeelen JH. 1989. Distribution of dynorphin B and methionine-enkephalin in the mouse hippocampus: influence of genotype. Neurosci Lett 97:241–244.

Wenzel HJ, Buckmaster PS, Anderson NL, Wenzel ME, Schwartzkroin PA. 1997. Ultrastructural localization of neurotransmitter immunoreactivity in mossy cell axons and their synaptic targets in the rat dentate gyrus. Hippocampus 7:559–570.

Witter MP, Amaral DG. 1991. Entorhinal cortex of the monkey: V. Projections to the dentate gyrus, hippocampus, and subicular complex. J Comp Neurol 307:437–459.

Witter MP, Van Hoesen GW, Amaral DG. 1989. Topographical organization of the entorhinal projection to the dentate gyrus of the monkey. J Neurosci 9:216–228.

Zappone CA, Sloviter RS. 2004. Translamellar disinhibition in the rat hippocampal dentate gyrus after seizure-induced degeneration of vulnerable hilar neurons. J Neurosci 24:853–864.

Zimmer J. 1971. Ipsilateral afferents to the commissural zone of the fascia dentata, demonstrated in decommissurated rats by silver impregnation. J Comp Neurol 142:393–416.